DIFFUSION[1]

1. INTRODUCTION

1.1 GRADIENT FLUX LAWS

In transport of contaminants in groundwater and soils solute exchange between mobile phase (here water) and the immobile phase (aquifer material, soil solids) depends on diffusion (e.g.: Rasmuson and Neretnieks, 1980; Rao et al., 1980; Wu and Gschwend, 1986). The same applies for technical systems e.g. for water treatment using activated carbon or ion exchange in fixed bed reactors (Crittenden et al., 1986; Weber and Smith, 1987; Nicoud and Schweich, 1989) or for adsorption of gases in microporous sorbents and catalysts (e.g., Kast, 1981). Slow diffusion may also be important during aquifer and soil remediation (e.g., pump&treat or soil air venting; e.g. Wilson, 1990). Mass transfer by diffusion is very similar to heat conduction, electrical conductivity, and flow of groundwater, as summarized in Table 1.1.

Table 1.1: Similarities of steady-state transport phenomena – gradient flux laws

The "gradient flux law"	**Flux** (Energy/Charge/Mass/Volume per Area per Time) = Transfer **Coefficient** x **Gradient** (Difference per Length)	**Coefficient**	**Units** x: Length [m]
Fourier, 1822	Heat flux $Q = - \lambda \Delta T/\Delta x$ [W m^{-2}; J m^{-2} s^{-1}]	λ: Heat conductivity [W K^{-1} m^{-1}]	T: Temperature [K; °C]
Ohm, 1827 1789-1854	Current (Ohm's law U = R I) $I = - k \Delta U/\Delta x$ [A m^{-2}; C m^{-2} s^{-1}]	k: Electrical conductivity [Ω^{-1} m^{-1}]	U: Electric potential, Voltage [V]
Fick, 1855 1829 – 1901	Mass flux $F = - D \Delta C/\Delta x$ [mol m^{-2} s^{-1}; g m^{-2} s^{-1}]	D: Diffusion coefficient [m^2 s^{-1}]	C: Concentration [mol l^{-1}; g l^{-1}]
Darcy, 1856 1803 – 1858	Volume flux (porous media) $Q = - K \Delta h/\Delta x$ [m s^{-1}; m^3 m^{-2} s^{-1}]	K: Hydraulic conductivity [m s^{-1}; m^3 m^{-2} s^{-1}]	h: Hydraulic potential [m]
Hagen[1]-Poiseuille[2] 1840 [1]1797-1884 [2]1797-1869	Volume flux (tubes) $Q = (\pi r^4)/(8 \eta) \Delta P/\Delta x$ (one tube)* [m^3 s^{-1}] $Q = r^2/(8 \eta) \Delta P/\Delta x$ (per tube area: πr^2) [m^3 m^{-2} s^{-1} = m s^{-1}]	r: Tube radius [m] η: Viscosity [Pa s = kg s^{-1} m^{-1}]	P: Pressure [Pa = N m^{-2} = J m^{-3} = m kg s^{-2} m^{-2}]

Fourier, J. (1822): Théorie Analytique de la chaleur, Firmion-Didot père et fils, Paris

Ohm, (1827): Die galvanische Kette, mathematisch bearbeitet (The Galvanic Circuit Investigated Mathematically). Berlin: Riemann, 1827. - 245 S

Fick, A. (1855): Poggendorff's Annalen. 94, 59-86 (Adolf Fick was working on Medical Physics on mixing of air in the lungs, work of the heart, heat economy of the body, muscular contraction, hydrodynamics of blood circulation; he is well known in the field of cardiology)

Darcy, H. (1856): Histoire des fontaines publiques de Dijon, Appendice, note D

* the pressure P may be replaced by the height difference Δh multiplied by the density of water (ρ_w = 1000 kg m^{-3}) and the gravitational constant (g = 9.81 m s^{-2}) which give Q as a function of the hydraulic gradient ($\Delta P = \Delta h \, \rho_w g$)

[1] This chapter comes to a large extent from the book: Diffusion in Natural Porous Media: Contaminant Transport, Sorption/Desorption and Dissolution Kinetics. Kluwer Academic Publishers, Boston, 224 p. (ISBN 0-7923-8102-5); Peter Grathwohl (1998)

1.2 NON-EQUILIBRIUM IN CONTAMINANT TRANSPORT

The fate of chemicals in the environment depends on their physicochemical properties (e.g., vapor pressure, water solubility, octanol/water partition coefficients, etc.) and the properties of environmental compartments encountered. Once introduced into the subsurface environment, spreading depends on the rates of mass transfer processes (e.g., advection, diffusion) in vapor and the aqueous phase, e.g., after a spill of hydrophobic organic compounds (Fig. 1.1). Diffusion is the most critical transport mechanism in low permeability zones (e.g., clay and silt layers/lenses at the macro-scale, hard rocks), porous aggregates and particles (grain scale) as shown in Fig. 1.2. Additionally, the interfacial mass transfer between non-aqueous phase liquids (NAPL) and groundwater or soil air also affect the long-term fate and transport of contaminants in soil and groundwater. Both, low permeability zones (places where organic contaminants accumulated over long periods) and NAPLs with low water solubilities can act as long-term sources of contamination.

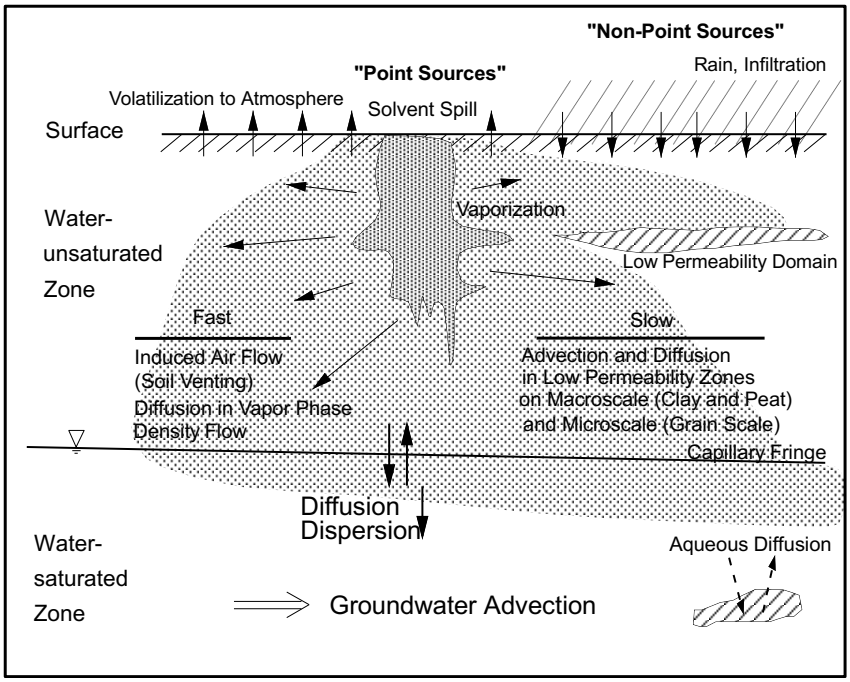

Fig. 1.1: Transport processes affecting the spreading of contaminants in the subsurface environment

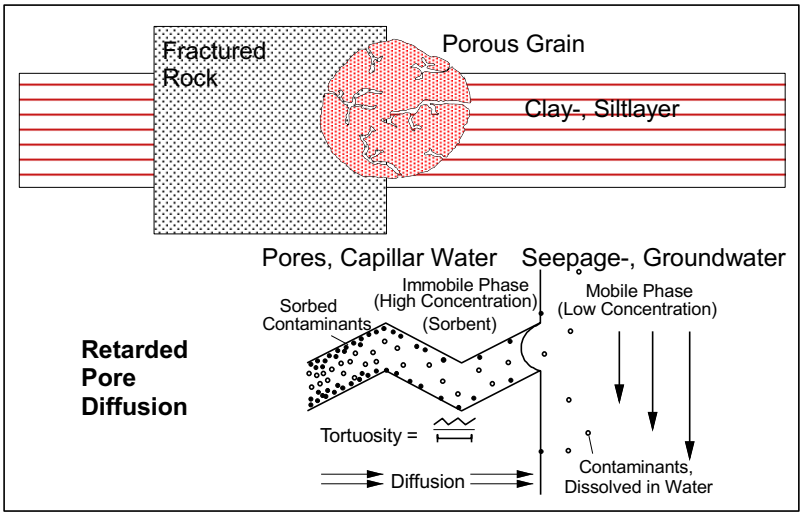

Fig. 1.2: Pore diffusion in porous media: sediment layers, rocks, porous particles, catalysts, etc.

Slow diffusion-limited sorption and desorption have a significant effect on advective contaminant transport in groundwater and the efficiency of soil remediation techniques. In field experiments of advective contaminant transport, retardation factors were found to increase with increasing migration distance (Roberts et al., 1986; Ptacek and Gillham, 1992), which was attributed to slow intraparticle pore diffusion (Ball and Roberts, 1991). Similarly, retardation factors were found to increase with decreasing flow velocities in column experiments (increasing residence time) as shown in Fig. 1.3 (Schüth and Grathwohl, 1994).

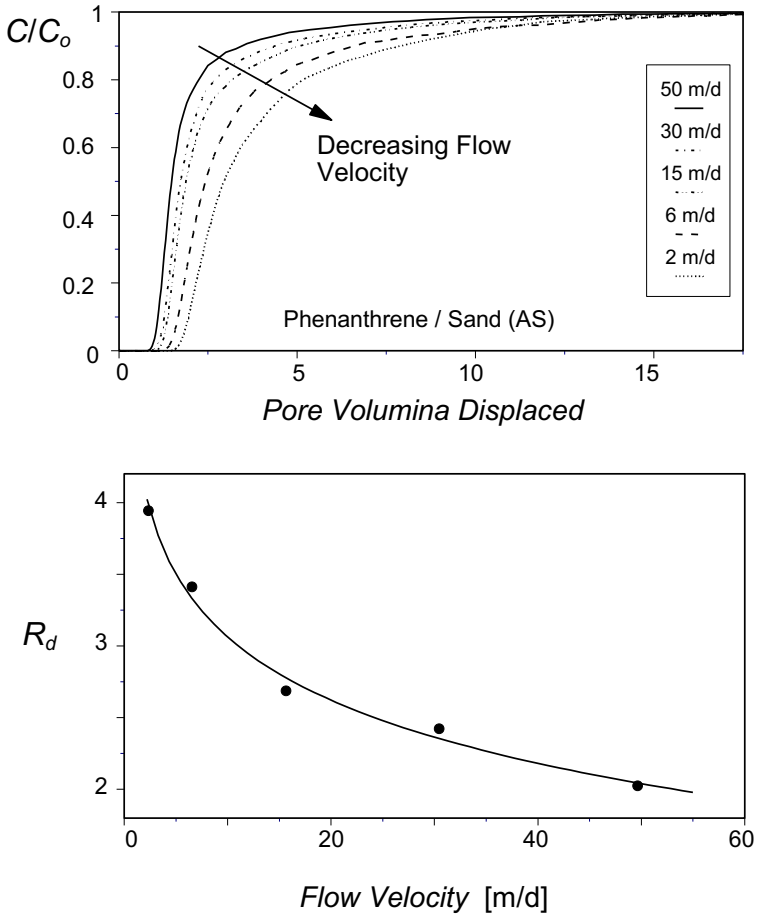

Fig. 1.3: Dependency of breakthrough times and retardation factors on contact time of phenanthrene in sand column experiments.

1.3 NON-EQUILIBRIUM IN CONTAMINANT REMOVAL

Slow, diffusion-limited removal rates also determine the effectiveness of soil remediation techniques (e.g., pump-and-treat, soil-air-venting). During the implementation of such remediation techniques, contaminant levels in the mobile zone (extracted air or groundwater) may initially decline very rapidly, but after a certain time contaminant levels often decline very slowly over very long-time periods, which is often described as "extended tailing" (Fig. 1.4).

Fig. 1.4 shows an example of "extended tailing" for a laboratory-scale soil-air-venting experiment. During the tailing part of the curve, the rate of removal becomes independent of soil air extracted (the same applies to contaminated sites where pump-and-treat is applied. Even differences in water content do not affect the removal rate in moist, water-unsaturated samples, indicating that diffusion in water-filled intraparticle pores is limiting the overall mass transfer rates (Grathwohl and Reinhard, 1992; 1993). When pump-and-treat or soil-air-venting is interrupted or

terminated, a rapid increase of the contaminant concentration is often observed in groundwater or soil air ("rebound").

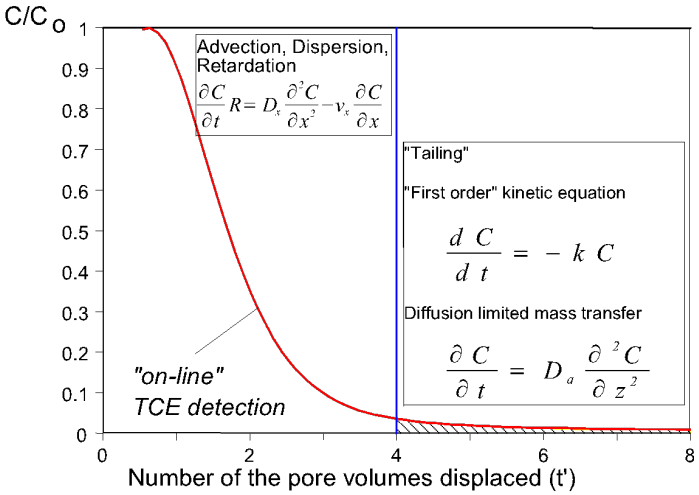

Fig. 1.4: Results from an experiment on soil vapor extraction: TCE release from contaminated sand.

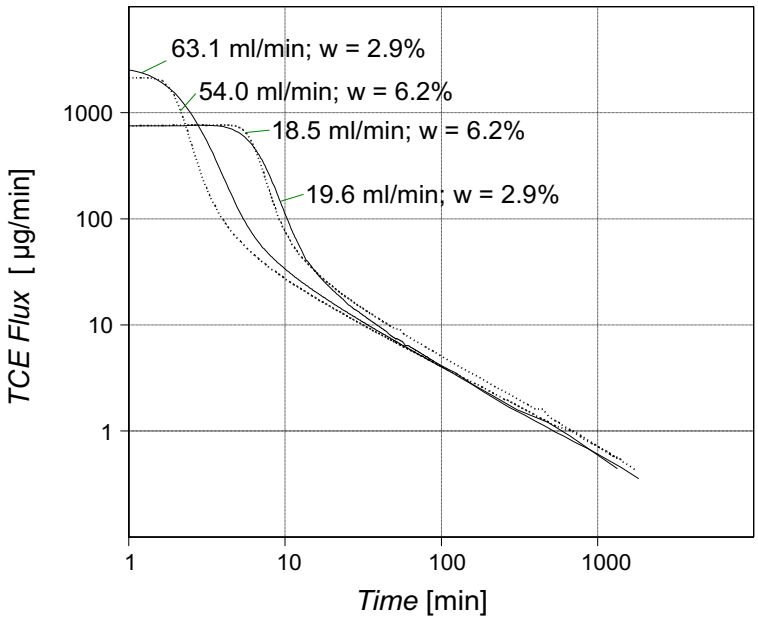

Fig. 1.5: "Tailing" after 10 min independent of the water content and the flow velocity.

1.4 MASS TRANSFER BETWEEN MOBILE/IMMOBILE PHASES

The general conclusion from the findings discussed above is that diffusion often affects or controls the overall rate of mass transfer between mobile and immobile phases. Fig. 1.6 shows a conceptual scheme of diffusive mass transfer between a particle and mobile phases for sorptive uptake and release of solutes. Mass transfer occurs across different interfaces (i.e.., water/air, NAPL/air/water, soil solids/water) limited by diffusion within a phase or two adjacent phases

(e.g., air, water, etc.). Mass transfer occurs when there is a fugacity (or concentration) gradient within a phase or between phases, e.g.:

if $f_{i(water)} > f_{i(air)}$,
if $f_{i(water)} > f_{i(solid)}$, or $f_{i(NAPL)}$, or
if $f_{i(water\ at\ point\ 1)} > f_{i(water\ at\ point\ 2)}$.

At equilibrium, all fugacities are equal ($f_{i(air)} = f_{i(water)} = f_{i(NAPL)} = f_{i(solid,\ sorbed)}$) and net mass transfer is zero. Under environmental conditions (ambient pressure, dilute concentrations), we can typically replace the fugacity gradient within one phase with a concentration gradient; different phases are connected by partitioning coefficients (e.g., Henry's law constant, $K_{oil/water}$, etc.).

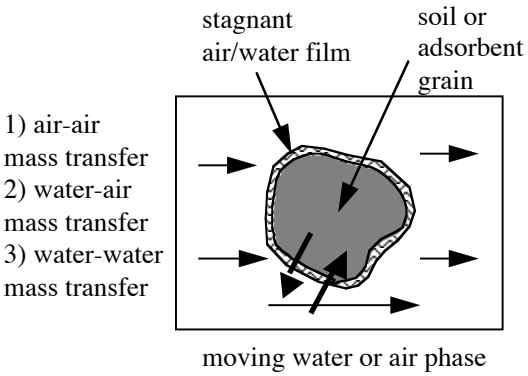

Fig. 1.6: Mass transfer at the grain scale

Fig. 1.7 shows a general scheme of interface mass transfer and concentration gradients. Groundwater or soil air represents the mobile phase, and the immobile phase consists of the soil solids, including stagnant water (adsorbed and pendular water as well as capillary water), or residual nonaqueous liquids. At larger scales, low permeability domains, such as clay or silt layers, allow only very limited advection of groundwater, and may also be considered as an immobile phase. In fractured rocks, matrix diffusion controls the mass transfer in the immobile phase (e.g., the disappearance and recovery of organic compounds in fractures).

In the vadose (unsaturated) zone relative humidities in the subsurface are close to 100% under field conditions, capillary condensation of water occurs in pores up to 0.1 μm in radius. Therefore, most intraparticle and intra-aggregate pores and pores in fine-grained sediments or rocks contain water, even in the vadose zone. Mass transfer in the immobile phase is limited by aqueous diffusion, which is about 10,000 times slower than diffusion in the vapor phase.

Diffusion across the stagnant water layer (film diffusion, as shown in Fig. 1.6) depends on hydrodynamic conditions. Especially for long-time scales, film diffusion can become negligible compared to pore diffusion in the matrix or particles. Mass transfer then primarily depends on diffusion in tortuous pores of sediment layers, rocks, intraparticle pores in sand and gravel, and in soil organic matter (intrasorbent diffusion, Brusseau et al., 1991) or a combination of intraparticle and intrasorbent diffusion. The rate of sorption/desorption is therefore limited by the diffusive transport of the solute to the sorption site. The process of adsorption or desorption of a molecule at the sorption site typically is much faster than transport to the sorption site.

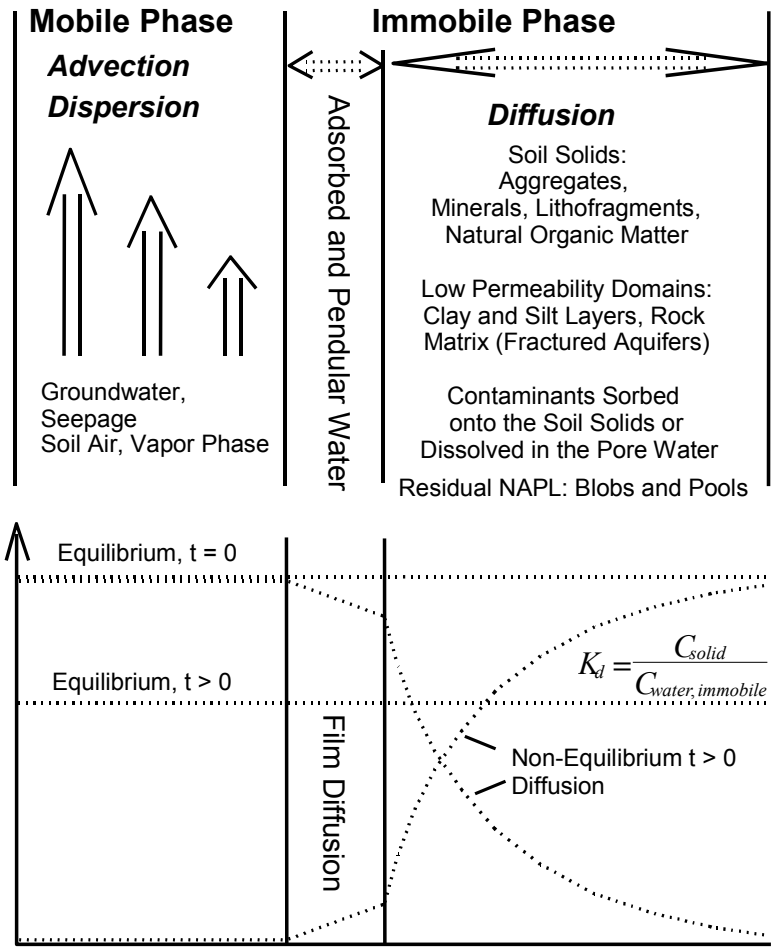

Fig. 1.7: Mobile-immobile phase mass transfer by film diffusion and pore diffusion as well as concentration gradients for uptake and release of solutes (e.g., transport to and from the sorption site in the immobile region as the reason for slow sorption/desorption).

2. DIFFUSION COEFFICIENTS

Diffusion coefficients depend on the mass and volume of the diffusing molecules, the temperature, and the medium in which diffusion takes place. Empirical correlations may be used for calculating diffusion coefficients. It should be noted that the application of such empirically derived equations (Eqs. 2.1 - 2.5) requires input parameters in specific units. The diffusion coefficient of non-polar gases in air (D_{air}) [L T^{-1}] at atmospheric pressure (~1 atm) and low to moderate temperatures T [K] may be estimated using the FSG (Fuller-Schettler-Giddings)-method (Lyman et al., 1990):

$$D_{air} = \frac{10^{-3} T^{1.75} \sqrt{1/m_{air} + 1/m_g}}{P\left(V_{air}^{1/3} + V_g^{1/3}\right)^2} \quad [\mathrm{cm^2/s}] \qquad (2.1)$$

V_{air}, V_g, m_{air}, and m_g denote the molar volumes [L^3] and average molecular masses [M mol^{-1}] of air and the diffusing gas, respectively (V_{air} = 20.1 cm^3/mol; m_{air} = 28.97 g/mol). P corresponds to the ambient pressure [atm]. Table 2.1 lists structural volume increments for the calculation of V_g for compounds.

Table 2.1: Atomic and structural diffusion volume increments to calculate molar volumes needed in Eq. 2.1 (V_g); according to Fuller et al. (1966).

Atom or structural segment	*ΔV_g [cm³/mol]*
Carbon	16.5
Hydrogen	1.98
Oxygen	5.48
Nitrogen	5.69
Chlorine	19.5
Sulfur	17.0
Aromatic and heterocyclic rings	-20.2

Molecular diffusion in liquids depends on the interactive forces between the molecules (e.g., solute and water, dilute solutions), which are accounted for as frictional drag. Diffusion coefficients in liquids are mainly affected by the dynamic viscosity (η) of the liquid (the viscosity of water at 293 K = 20°C is: 1.002E-3 N·s/m² = kg·m⁻¹·s⁻¹ = Pa·s = J·s/m³ = 1.002 centipoise). In dilute solutions, the diffusion coefficients are virtually independent of the composition. Several methods are available to calculate liquid diffusion coefficients. For spherical molecules, which are much larger than the solvent molecules (macromolecules, colloids), or particles of effective molecular radius r_m, the diffusion coefficients can be determined by the Stokes-Einstein equation (Atkins, 1985):

$$D_{aq} = \frac{K_B T}{6\,\pi\, r_m\, \eta} \tag{2.2}$$

where K_B denotes the Boltzmann constant (1.38066E-23 J K^{-1}). For the calculation of diffusion coefficients of small organic molecules in dilute aqueous solutions, Wilke and Chang (1955) developed a widely used empirical correlation:

$$D_{aq} = \frac{7.4E-08\; T\sqrt{X m_{sol}}}{\eta V'^{0.6}}\ \ [\mathrm{cm^2/s}] \tag{2.3}$$

where η is expressed in units of centipoise. X denotes an empirical association parameter of the solvent (= 2.6 for water and = 1 for nonpolar fluids), and m_{sol} is the molecular weight of the solvent. V' [cm³/mol] denotes the (Le Bas) molar volume of the diffusing substance (at boiling point), which may be estimated from Kopp's law of additive atomic volumes (see Satterfield, 1970) using the values in Table 2.1 and 2.2, respectively. As an example, the calculation of the molar volume of trichloroethene is given in Box 2.1. For further examples, see Lyman et al., 1990; p. 17-11, Table 17.5. As a first approximation of V' and V_g, the molar volume of the liquid substance may be used (e.g., the ratio of the liquid density and the molecular weight of the solute).

Hayduk and Laudie (1974) further developed the Wilke and Chang correlation and suggested slightly different constants based on D_{aq} measured for 89 organic compounds:

$$D_{aq} = \frac{13.26E-05}{\eta^{1.14} V'^{0.589}}\ [\mathrm{cm^2/s}] \tag{2.4}$$

Table 2.2: Additive (atomic) volume increments ($\Delta V'$) for the estimation of the molar volume (V') at the normal boiling point temperature (from Satterfield, 1970); for use in Eqs. 2.3 and 2.4

Atom or structural segment	*$\Delta V'$ [cm³/mol]*
Carbon	14.8
Hydrogen	3.7
Oxygen, generally	7.4
in methyl esters and ethers	9.1
in ethyl esters and ethers	9.9
in higher esters and ethers	11.0
in acids	12.0
jointed to S, P, N	8.3
Nitrogen, doubly bonded	15.6
in primary amines	10.5
in secondary amines	12.0
Bromine	27.0
Chlorine	24.6
Fluorine	8.7
Iodine	37.0
Sulfur	25.6
Ring, three-membered	-6.0
four-membered	-8.5
Five-membered	-11.5
Six-membered	-15.0
naphthalene	-30.0
anthracene	-47.5

* the additive-volume method of obtaining *V'* should not be used for simple molecules like H_2, O_2, CO_2, H_2O, NH_3, etc.

Box 2.1: Example for the Calculation of TCE Diffusion Coefficients in Air and Water

1. Calculation of the molar volume in air according to Fuller et al., 1966:

$V_{g,TCE} = 1\Delta V_{g,H} + 2\Delta V_{g,C} + 3\Delta V_{g,CI}$

= 1·1.98 + 2·16.5 + 3·19.5 (values from Table 2.1)

= 93.5 cm³/mol

2. Calculation of the molar volume in water according to Kopp's Law:

$V'_{TCE} = 1\Delta V'_H + 2\Delta V'_C + 3\Delta V'_{CI}$

= 1·3.7 + 2·14.8 + 3·24.6 (values from Table 2.2)

= 107.1 cm³/mol

3. Approximation the molar volume in air or water from the ratio of the liquid density and the molecular weight of TCE:

$V_{TCE} = m_{TCE}/\rho_{TCE} = 131.5/1.465 = 89.8 cm^3/mol$

TCE-diffusion coefficients in air and water calculated from the different values of $V_{g,TCE}$, and V'_{TCE} according to the FSG-method (Eq. 2.1) and to Wilke and Chang, 1955 (Eq. 2.3) at 20°C:

	Molar Volume [cm³/mol]	*D_{air} [cm²/s] at 20°C*	*D_{aq} [cm²/s] at 20°C*
Fuller et al.:	93.5	8.09 E-02	-
Kopp's Law:	107.1	-	8.97 E-06
Approx. (m/ρ):	89.8	8.23 E-02	9.97 E-06

The empirical exponent of viscosity (centiPoise in Eq. 2.4) also considers the variability of diffusion with changing temperature. Thus, the temperature is not explicitly included in Eq. 2.4. Worch (1993) derived the following simple relationship, which is based on the viscosity (in

centiPoise), the temperature, and the molecular weight (more readily accessible than the molar volume) of the diffusing substance (m_s):

$$D_{aq} = \frac{3.595E-7\,T}{\eta\, m^{0.53}}\ [\mathrm{cm^2/s}] \qquad (2.5)$$

In Fig. 2.1, the different methods of calculating temperature-dependent diffusion coefficients in air and water are compared for trichloroethene (as one example for hydrophobic organic compounds). Since the viscosity of a fluid decreases with increasing temperature, diffusion in liquids shows a stronger dependency on temperature than diffusion in the vapor phase. Table 2.3 shows calculated and observed diffusion coefficients of some common organic contaminants in air and water. Since the viscosity of liquids depends on the temperature exponentially (Arrhenius law), the increase of aqueous diffusion coefficients with temperature can also be described by an Arrhenius type of relationship.

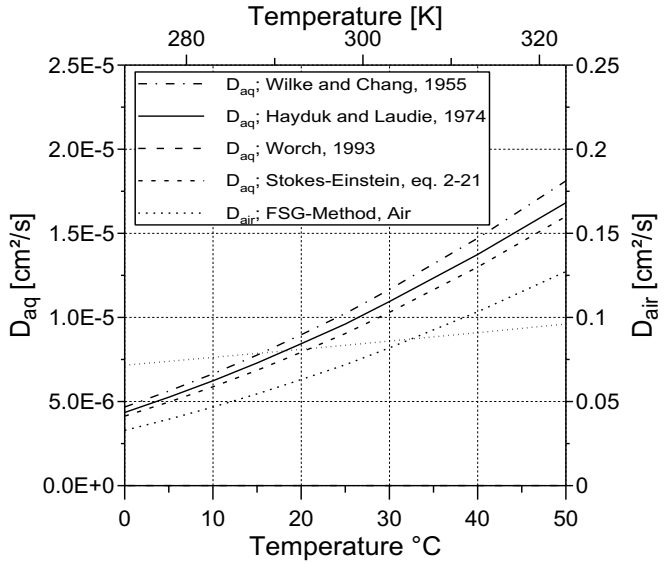

Fig. 2.1: Diffusion coefficients of Trichloroethene (TCE) in air (Eq. 2.1) and water (Eq. 2.2 to 2.5) *vs*. temperature. Calculations based on $V_{g,TCE}$ = 93.5 cm³/mol; V_{TCE} = 107.1 cm³/mol; m_{TCE} = 131.51 g/mol; r_{TCE} = 3.4 nm).

Table 2.3: Calculated diffusion coefficients in air (D_{air}: Eq. 2.1, FSG-method) and water (D_{aq}: Eq. 2.4, Hayduk and Laudie) of some selected organic contaminants (all data at 25°C; values in parentheses are measurement in air by Lugg, 1968 and in water by Hayduk and Laudie, 1974)

Compound	D_{air} [cm²/s]	D_{aq} [cm²/s]
Methanol	0.162 (0.152)	1.8 (1.66)E-05
Vinylchloride	0.11	1.29 (1.34)E-05
Dichloromethane	0.105 (0.104)	1.22E-05
Trichloroethene	0.0833 (0.0875)	0.960E-05
Perchloroethene	0.076 (0.0797)	0.865E-05
Benzene	0.094 (0.0932)	1.02 (1.09)E-05
Toluene	0.0804 (0.0849)	0.906 (0.950)E-05
o-Xylene	0.0735 (0.0727)	0.819E-05
m-Xylene	0.0735 (0.0688)	0.819E-05
para-Xylene	0.0735 (0.067)	0.819E-05
Naphthalene	0.0702	0.795E-05
Phenanthrene	0.0597	0.671E-05
Benzo(a)pyrene	0.0513	0.563E-05
Pentachlorophenol	0.0592	0.650E-05

3. STEADY STATE DIFFUSION IN POROUS MEDIA: THE EFFECTIVE DIFFUSION COEFFICIENT

Solute diffusion in natural porous media is hindered by the tortuous nature of the pores, the diminished cross-sectional area available for diffusion, and possibly by the pore sizes (i.e., overall heterogeneity of the subsurface). Under steady-state conditions, the mass flux depends on the concentration gradient and is expressed by Fick's 1st law:

$$F = -D_e \frac{dC}{dx} \tag{3.1}$$

Under water-saturated conditions, C refers to the solute concentration in the pores [M L^{-3}]. D_e denotes the effective diffusion coefficient [L^2 T^{-1}] and is defined as:

$$D_e = \frac{D_{aq}\varepsilon_t\delta}{\tau_f} \tag{3.2}$$

τ_f and δ are dimensionless factors accounting for tortuosity (> 1) and constrictivity (≤ 1) of the pores, respectively. ε_t is the effective transport-through porosity, which accounts for the reduced cross-sectional area available for diffusion when diffusion occurs only in the pore space (no solids diffusion). ε_t can be smaller than the overall porosity of the medium if the porous medium contains small pores, which are not accessible for the solute (size exclusion, restricted diffusion) and pores that do not contribute to the overall solute transport (e.g., dead-end or blind pores) (Lever et al., 1985).

Restricted Diffusion. In water-saturated porous media, diffusion depends on intermolecular collisions (e.g., water molecules - solute molecules). Pore diffusivity is identical to the molecular diffusivity, as long as the pores are large compared to the mean free path of a molecule (Λ). Note, that Λ is the distance traveled between collisions (1-2 times the molecular diameter in liquids and ~ 70 times the molecular diameter in gases). If pore sizes approach the mean free path so-called Knudsen diffusion may occur. If pore sizes in most natural porous media are much larger than the mean free path in water of about 1 nm, Knudsen diffusion is negligible (Kärger and Ruthven, 1992).

In narrow liquid-filled pores, the value of D_e can decrease, if there is a drag due to a greater viscosity of the solvent. This increase in viscosity, compared to the bulk viscosity of the solvent, is caused by the proximity of the pore wall (Cussler, 1984). This is typically applicable to small pores and narrow pore throats, which have diameters with the same order of magnitude as the diffusing molecules. The constrictivity factor (δ) accounts for this steric hindrance effect. δ depends on the ratio of the solute diameter to the pore diameter (λ_p):

$$\lambda_p = \frac{molecule\ diameter}{pore\ diameter} < 1 \tag{3.3}$$

δ may be quantified by empirical equations, as developed by Renkin (1954), Beck and Schultz (1970), Satterfield and Colton (1973), and Chantong and Massoth (1983):

$$\delta = (1-\lambda_p)^2(1 - 2.104\lambda_p + 2.09\lambda_p^3 - 0.95\lambda_p^5) \tag{3.4}$$

$$\delta = (1-\lambda_p)^4 \tag{3.5}$$

$$\delta = \exp(-4.6\lambda_p) \tag{3.6}$$

$$\delta = 1.03\exp(-4.5\lambda_p) \tag{3.7}$$

Eqs. 3.4 and 3.5 are based on steady-state diffusion of organic solutes (e.g., urea, glucose, sucrose, raffinose) through membranes (e.g., cellulose sausage casings/cellophane sheets and mica membranes) (Renkin, 1954; Beck and Schultz, 1970). Eqs. 3.6 and 3.7 are based upon transient diffusion of nonaromatic and aromatic compounds in silica-alumina beads (Satterfield and Colton, 1973), and diffusion of polyaromatic compounds in aluminas of known pore size (Chantong and Massoth, 1983). According to Beck and Schultz (1970), the first term on the right-hand side in Eq. 3.4 (Renkin-Equation) represents an exclusion of solute from the membrane pores based on geometrical considerations. The second term represents the additional hydrodynamic drag on the solute molecules due to the proximity of the pore walls.

Fig. 3.1 shows a comparison of the equations given above (Eqs. 3.4 - 3.7). Although Eqs. 3.4 through 3.7 were derived for different compounds in different systems, these empirical correlations agree very well. For most organic contaminants (molecular diameter < 1 nm), a significant contribution is expected if λ_p is greater than 0.1 (pore diameter < 10 nm). Therefore, restricted diffusion of most organic contaminants of interest is expected in the micropore and lower mesopore range. The definition of pore sizes here follows the IUPAC (International Union of Pure and Applied Chemistry) pore classification, as shown in Box 3.1 (Sing et al., 1985). The situation may become different for charged species and charged surfaces. For example, clay minerals typically have negatively charged surfaces which leads to the formation of electrical double layers and anion exclusion. This is relevant for radioactive waste disposal and diffusion of radionuclides (e.g. $^{129}I^-$, $^{36}Cl^-$) in clay formations (Charlet et al., 2017; van Loon et al., 2023).

Box 3.1: IUPAC (International Union of Pure and Applied Chemistry) Definition of Pores Sizes

micropores:	pore width	< 2 nm
mesopores:	pore width	2 nm - 50 nm
macropores:	pore width	> 50 nm

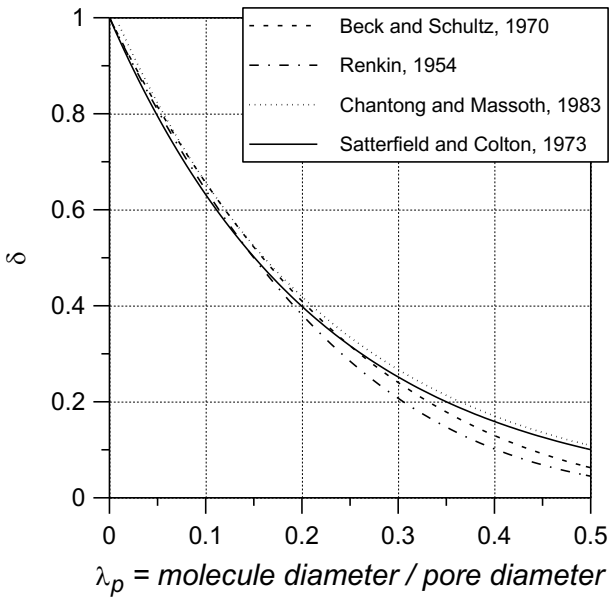

Fig. 3.1: Constrictivity factor (δ) versus relative pore size.

Tortuosity. The tortuosity factor τ_f in Eq. 3.2 accounts for the pore geometry and is defined as the square of the ratio of the effective path length l_e in the pore to the shortest distance l in a porous medium:

$$\tau_f = \left(\frac{l_e}{l}\right)^2 > 1 \qquad (3.8)$$

According to Dullien (1991) τ_f is not necessarily a property of the porous medium, but a parameter of the one-dimensional capillary model of the medium (see Box 3.2). The capillary model of a porous medium assumes a number of parallel pores as a substitute for the tortuous pores. The porosity of the model must match the porous medium porosity. Therefore, the number of pores in the capillary model is increased by a factor of l_e/l. Consequently, l_e/l is squared $(l_e/l)^2$ in the definition of D_e (Epstein, 1989).

Box 3.2. Derivation of the Tortuosity Factor $\left(\tau = l_e/l\,;\tau_f = (l_e/l)^2\right)$

1. Steady-State Diffusion

Diffusion through a non-porous medium (e.g. water)

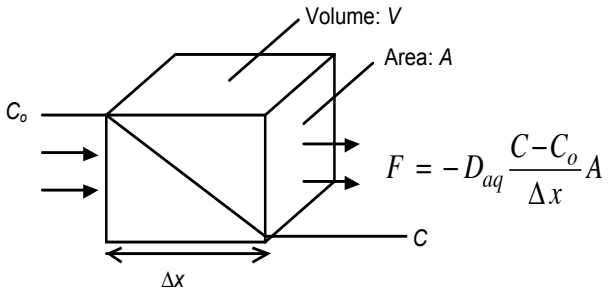

2. Capillary Bundle Model of Porous Media

Diffusion through a bundle of straight tubes (cross sectional area of all tubes: ∅; length: *l*)
Volume: *V*; Pore Volume: ∅ *l* ; Porosity: ε = (∅ *l*)

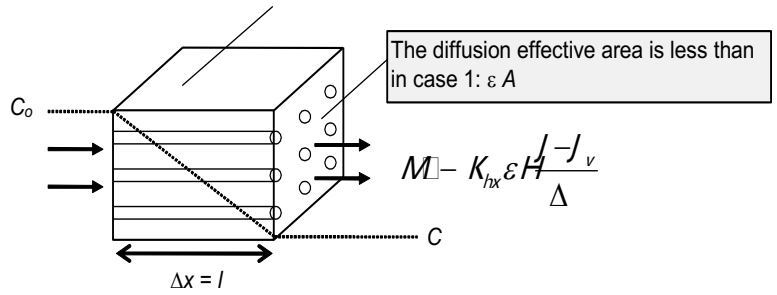

3. "Real" Porous Medium

Diffusion through tortuous pores (cross sectional area of all tubes: ∅; length: l_e)

Volume: *V*; Pore Volume: ∅ l_e ; Porosity: ε = (∅ l_e) / *V*

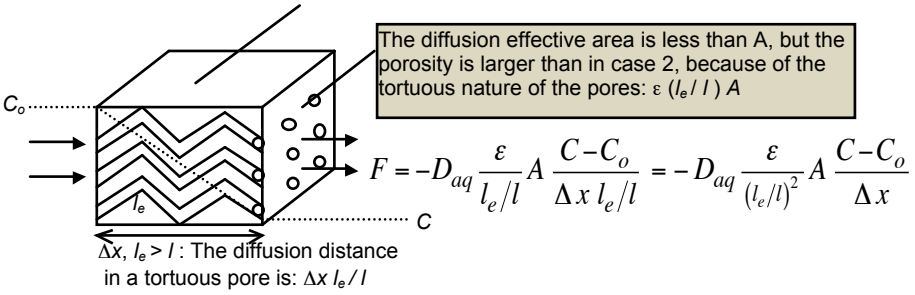

➔ Tortuous pores result in an increased porosity and an increased effective diffusion distance compared to the capillary bundle model: both have to be considered in the definition of the D_e or τ_f, respectively.

τ_f, as defined in Eq. 3.8, is only valid if the capillary diameter of the model is representative of the effective pore diameter of the porous medium. Peterson (1958) showed that diffusion in pores of varying cross-sections (i.e., varying radii) might result in abnormally large tortuosity factors. Dykhuizen and Casey (1989) showed that inhomogeneous, isotropic porous media, the tortuosity factor equals 3. In natural porous media, this condition of homogeneity and isotropy is rarely achieved, and the tortuosity factor serves as a "correction factor".

In most cases, only the overall porosity (ε) of porous media can be determined easily (pore size distributions and tortuosities are unknown). Thus, the relative diffusivity ($D' = D_e/D_{aq}$) is defined as an empirical function of ε alone (δ = 1):

$$D_e = D_{aq}\varepsilon^m \Longrightarrow \varepsilon^m = \frac{\varepsilon}{\tau_f} = \frac{D_e}{D_{aq}} = D' \tag{3.9}$$

where m is an empirical exponent. Eq. 3.9 is analogous to Archie's law, which is an empirical correlation describing the electrical conductivity in porous rocks (Archie, 1942). The concentration gradient, which gives rise to the diffusive flux, is analogous to the electrical field (Klinkenberg, 1951). The conductivity of porous material (e.g., brine saturated rocks) is:

$$\sigma_{rock} = a_f\sigma_{aq}\varepsilon^m; F_f = \frac{1}{a_f\varepsilon^m} = \frac{\sigma_{aq}}{\sigma_{rock}} \tag{3.10}$$

where σ_{rock} and σ_{aq} denote the electrical conductivities (Sm L^{-1}) of the rock and the pore water, respectively. The formation factor F_f denotes a dimensionless resistance; a_f is an empirical factor, which, according to Thompson et al. (1987), should be unity. Archie's law may also be expressed in terms of relative conductivity. If a_f equals 1, Eq. 3.10 is equivalent to Eq. 3.9 $\left(\sigma' = \sigma_{rock}/\sigma_{aq} = \varepsilon^m\right)$.

The electrical conductivity of brine-saturated rocks is used to estimate the permeability of rocks (e.g., Taherian et al., 1990). The empirical exponent m of sedimentary rocks is also known as the cementation factor. Values of m, as reported in the literature, can vary significantly. Ullman and Aller (1982) found that the formation resistivity factors in nearshore sediments are correlated with the inverse of the porosity squared (m = 2).

Archie (1942) found that the exponent m varied between 1.8 and 2.0 in consolidated materials. In unconsolidated sand, he found a value of 1.3. For an isotropic packing of spherical particles, a theoretical value of $m = 3/2$ was derived (Bruggeman, 1935). Adler et al. (1992) reported a value of m = 1.64 for Fontainebleau sandstone. In diffusion experiments with silver catalyst pellets (Wakao and Smith, 1962) and sedimentary rocks (sandstones and limestones; Grathwohl, 1992), values of m close to 2 were observed. Probst and Wohlfahrt (1979) found that m equals 1.43 for loose packings of catalyst particles, which is close to the relationship reported by Bruggeman (1935) for the electrical conductivity of composites. Millington and Quirk (1960) reported a value of $4/3$ for the diffusive flow of gases at normal pressures or diffusion of ions in solution in soils. In experiments on the diffusion of gases through compacted sands, a value of m = 1.5 was determined (Shimamura, 1992). According to Thompson et al. (1987), each rock-pore geometry yields a distinct exponent, and m is predictable only for a particular pore geometry. Generally, in materials of low porosities (e.g., < 0.2), larger values of m (≥ 2) were observed (Wong et al., 1984; Boving and Grathwohl, 2001).

Attempts have been made to explain Archie's law from theoretical principles: (1) based on percolation models) (Shanthe and Kirkpatrick, 1971; Kirkpatrick, 1973; Wagner and Balberg, 1987); (2) effective-medium theories (Burganos and Sotirchos, 1987); (3) fractal pore structures

(Cushman, 1991); and (4) the statistical physics of sedimentary rocks (Wong, 1988; Guegen and Dienes, 1989). Balberg (1986) found that "a broad range of observed *m* values is consistent with expectations from ordinary percolation theory" - *m* depends on the dimensionality, the pore neck size distributions, and the degree of anisotropy of the percolation system. According to Katz and Thompson (1985), Archie's law follows directly from the self-similar nature of a specific pore geometry, even for the lowest porosities. Yet, no universal Archie's law exponent exists.

Sen et al. (1984) found that the dielectric constant depends on the rock texture and not on the porosity alone. If the porous medium consists of non-spherical particles (cylinders, disks), *m* depends on their orientation and shape (Sen et al., 1981). An orientation of plate-like grains or ellipsoids with their axis perpendicular to the electrical field (concentration gradient) results in a value of *m* larger than 1.5, whereas a parallel alignment results in a value of *m* smaller than 1.5 (*m* = 1.5 for spheres). For example, Sen et al. (1981) reported a value of *m* = 1 for needles and disks oriented parallel to the field, *m* = 2 and *m* >> 2 (e.g., 10) for cylinders and plates oriented perpendicular to the field, respectively.

Fig 3.2 shows a few simple D' - ε relationships, as discussed above. It also includes Maxwell's equation (Maxwell, 1873) for conductivity (σ') or diffusivity in rocks (D'):

$$D' = \frac{2\varepsilon}{3-\varepsilon} \tag{3.11}$$

Similar relationships, as discussed above, were developed for vapor phase diffusion in the water-unsaturated zone (see later), for the diffusion of gases in catalysts (for a review, see Probst and Wohlfahrt, 1979), and for the diffusion of sulfate and methane in marine sediments (Iversen and Jørgensen, 1993).

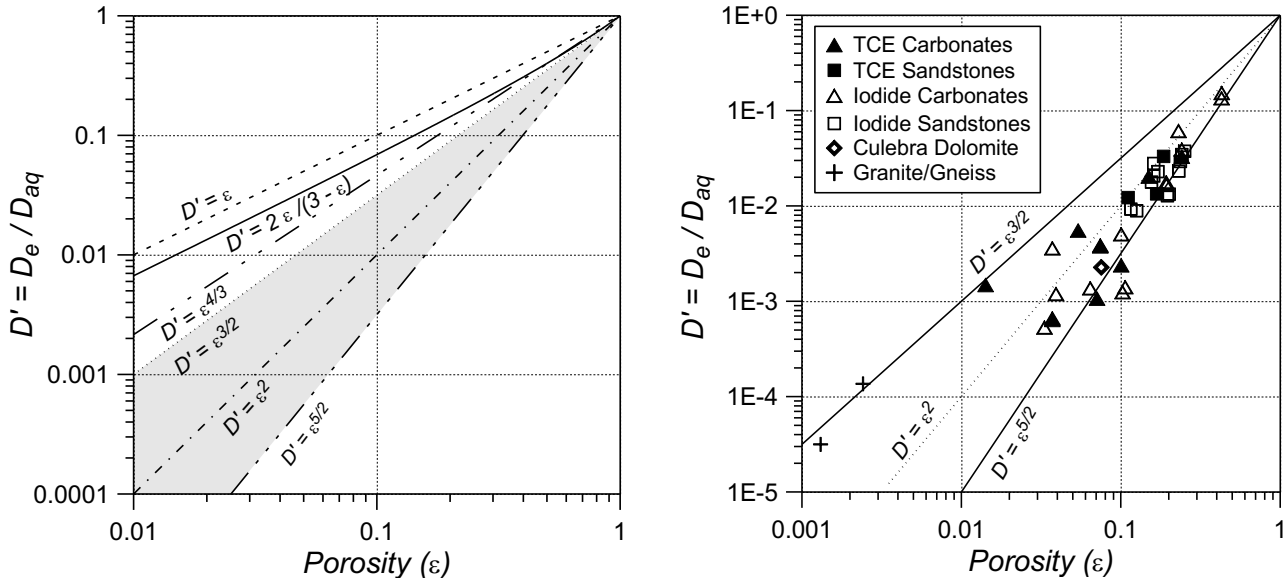

Fig. 3.2: Comparison of some D' - ε relationships (the shaded area denotes the range expected for most natural porous media) and some measured data (Boving and Grathwohl, 2001; here *m* is close to 2.2)

It should be noted that D' and *m* depend solely on the properties of the porous medium. They should therefore be independent of temperature, sorption capacities of the porous media, and the properties of the solute (i.e., the same values for different solutes). In random systems with a broad distribution of pores, both D_e and *F* may be dominated by a small fraction of well-connected pores or those pores with very high conductance (Thompson et al., 1987).

4. TRANSIENT DIFFUSION: THE APPARENT DIFFUSION COEFFICIENT

4.1 RETARDED PORE DIFFUSION

Transient diffusion generally is described by Fick's 2nd law:

$$\frac{\partial C}{\partial t} = D\frac{\partial^2 C}{\partial x^2} \tag{4.1}$$

where C denotes a concentration in a bulk volume. In a two-phase system (e.g. a water-saturated porous media where the solute is subject to sorption), we have to account for concentration changes in solids ($\partial C_s/\partial t$) and water ($\partial C_w/\partial t$). C_s and C_w usually have different units, and we have to account for the dry bulk density ($\rho = (1 - \varepsilon)\, d_s$; d_s is the density of the solid [M L^{-3}]) and the water-filled pore volume (porosity ε). If local equilibrium between solids and liquid exists (sorption at an internal site is fast compared to the diffusion process), the distribution coefficient ($K_d = C_s/C_w$) can be applied:

$$\rho\frac{\partial C_s}{\partial t} + \varepsilon\frac{\partial C_w}{\partial t} = \frac{D_{aq}\varepsilon_t}{\tau_f}\frac{\partial^2 C_w}{\partial x^2} = D_e\frac{\partial^2 C_w}{\partial x^2}$$

$$\frac{\partial C_w}{\partial t}(\varepsilon + K_d\,\rho) = D_e\frac{\partial^2 C_w}{\partial x^2} \tag{4.2}$$

$$\frac{\partial C_w}{\partial t} = \frac{D_e}{(\varepsilon + K_d\,\rho)}\frac{\partial^2 C_w}{\partial x^2}$$

The gradient on the right-hand side is the same in water, solid or bulk phase (local equilibrium). The term ($\varepsilon + K_d\rho$) is a capacity factor (α) of the porous medium (e.g., rock capacity factor). The ratio D_e/α is the apparent diffusion coefficient, D_a, which applies under transient conditions:

$$D_a = \frac{D_{aq}\varepsilon_t}{(\varepsilon + K_d\,\rho)\tau_f} = \frac{D_e}{\alpha} \tag{4.3}$$

Dead end or blind pores are not accounted for in the effective transport-through porosity (ε_t), whereas such pores (included in the overall porosity ε) may also represent a sink for the solute (and thus are included in the capacity term). Constrictivity is neglected in Eq. 4.3. In most cases, ε_t equals ε, and a simple retardation factor R_p for pore diffusion may be defined:

$$R_p = \frac{\alpha}{\varepsilon} = 1 + K_d\frac{\rho}{\varepsilon} \tag{4.4}$$

The definition of R_p is analogous to the retardation factor used to describe the advective transport of solutes in groundwater at equilibrium conditions. Hence, D_a may be interpreted as a retarded pore diffusion coefficient:

$$D_a = \frac{D_p}{R_p} \tag{4.5}$$

where D_p denotes the pore diffusion coefficient (D_{aq}/τ_f). If no sorption of the solute occurs in the porous medium ($K_d = 0$; conservative, non-reactive tracer), R_p is 1, and D_a equals D_p. If sorption is nonlinear, the distribution coefficient K_d depends on the concentration, and therefore, D_a also becomes a concentration-dependent quantity. As a first, linear approximation for a Freundlich type nonlinear sorption isotherm, D_a for a specific concentration range (described by a

representative concentration C) can be estimated by a linear approximation of K_d from a Freundlich isotherm:

$$D_a = \frac{D_e}{\left(\varepsilon + \rho\, K_{Fr} C_w^{1/n-1}\right)} \tag{4.6}$$

D_a here is a bulk diffusion coefficient representative for whole concentration profile at the front (i.e. allows to calculate the progress of the front position). Implicit numerical solutions of the transport equation with nonlinear sorption use the derivative of the Freundlich sorption isotherm.

Fig. 4.1 shows the concentration dependency of D_a and R_p, respectively, for Freundlich sorption isotherms with different degrees of nonlinearity. Eq. 4.6 can be used to calculate a value for D_a, which may be assumed to be constant within a limited concentration range. Since the concentrations change with time during diffusion limited sorption or desorption in the case of nonlinear sorption, D_a appears as a time-dependent parameter.

If ε is small compared to ρ K_{Fr} (e.g. 0.1 and 24, respectively; see dashed line in Fig. 4.1), R_p and $1/D_a$ depend solely on $C^{1/n-1}$, and will decrease with increasing concentrations for $1/n < 1$ and vice versa.

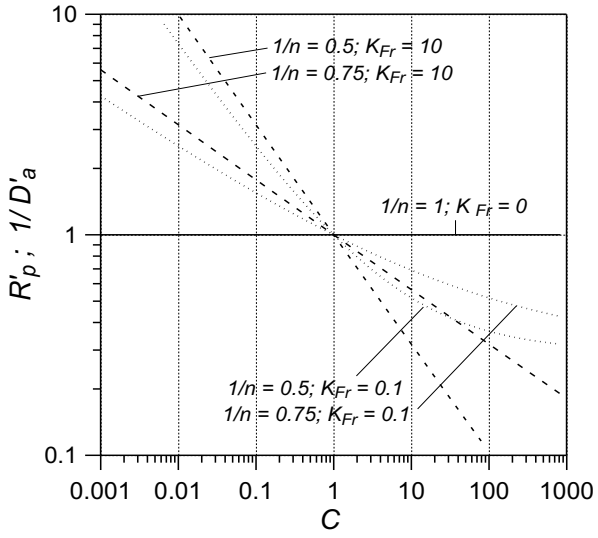

Fig. 4.1: Impact of nonlinear Freundlich sorption isotherms on retardation and diffusivity (R'_p and $1/D'_a$ are normalized: $\left(\varepsilon + \rho K_{Fr} C^{1/n-1}\right)/(\varepsilon + \rho K_{Fr})$. ε and ρ in this example are 0.1 and 2.4, respectively.

4.2 SURFACE DIFFUSION

Surface diffusion in an adsorption layer on the pore walls may result in an additional mass transfer in the direction of decreasing surface concentration (Bhatia, 1988). It may contribute to the overall diffusive transport in porous media only if appreciable adsorption of the solute onto internal surfaces occurs. The adsorbed molecules are still mobile (chemisorbed species are nearly immobile). Surface diffusion is commonly observed in adsorption of vapors in porous adsorbents (Klotz and Rousseau, 1988) and in strong adsorbents such as activated carbons (Sontheimer et al., 1985). The contribution of surface diffusion to the overall diffusion increases if the attractive forces from the surface decrease with adsorption in multimolecular layers compared to monomolecular layers (Kast, 1988). Therefore, surface diffusion becomes significant above a threshold concentration. The diffusive flux due to surface diffusion increases with increasing sorption; Fick's 2nd law may then be written as:

$$\frac{\partial C_w}{\partial t} = \frac{D_e + D_{s,e} K_d \rho}{(\varepsilon + K_d \rho)} \frac{\partial^2 C_w}{\partial x^2} \tag{4.7}$$

where $D_{s,e}$ denotes an effective surface diffusion coefficient. Surface diffusion depends on the concentration (Aris, 1983) and on the rates of adsorption and desorption (Riekert, 1985).

Distinguishing between the contribution of surface diffusion and pore diffusion is difficult because both processes co-occur. An additional mass transfer due to surface diffusion would result in tortuosity factors, which are too low if calculated according to Eq. 4.3. Evidence for surface diffusion in aqueous systems (e.g., water-saturated natural porous media) is limited. Komiyama and Smith (1974) reported that surface diffusion is a major contributor to the intraparticle transport of benzaldehyde in liquid-filled pores of Amberlite™ particles (polystyrene). Seidel and Carl (1989) found that surface diffusion is concentration-dependent in sorptive uptake of phenol and indole in activated carbon.

Diffusion in surface coatings (e.g., organic films adsorbed onto the pore walls) may also be interpreted as a process analogous to surface diffusion. In natural porous media, organophilic pores (i.e., pores with organic coatings) were found to contribute significantly to the steady-state diffusive fluxes of hydrocarbons (Yariv, 1976; Thomas and Clouse, 1990a). Based on diffusion coefficients measured in kerogens, Thomas and Clouse (1990b/c) concluded that diffusive fluxes of hydrocarbons could account for small to moderate fossil fuel accumulations. Mass transfer, in this case, occurs by diffusion in parallel in the organic and aqueous phases:

$$\mathrm{F} = -\left(\frac{D_{aq}\varepsilon_{aq}}{\tau_{aq}} + \frac{D_o\varepsilon_o K_o}{\tau_o}\right)\frac{dC_w}{dx} \tag{4.8}$$

ε_{aq}, ε_o, τ_{aq}, τ_o, D_o, and K_o denotes the volumetric fractions of water and organic phase per unit volume rock, the tortuosity factors in water and organic phase, the diffusion coefficient, and the volumetric partition coefficient of the solute in the organic phase, respectively.

If the solute shows significant partitioning (which especially applies for strongly hydrophobic organic solutes), then higher fluxes in the organic phase compared to the aqueous phase may occur. This flux occurs because of steep concentration gradients in the organic phase despite the much lower diffusion coefficients in the highly viscous organic phase than in water.

In the transport of contaminants in soils and sediments, where the organic matter contents are low, the mass transfer rates observed are generally too small (tortuosity factors too high) to allow for an interpretation of mass transfer as surface diffusion. However, in natural organic matter (e.g. coals or kerogenes) and bituminous shales, such effects might occur.

4.3 DIFFUSION IN NATURAL ORGANIC MATTER - ORGANIC POLYMERS

In humic soils that contain particulate organic matter (e.g., plant residues, coals), diffusion also occurs in the soil organic matter. For example, Nkedi-Kizza et al. (1989) concluded from displacement experiments of hydrophobic organic chemicals and ^{45}Ca in soil columns that nonequilibrium sorption was due to an intrasorbent (intra-organic matter) diffusion mechanism. The real structure of the natural organic matter is unknown. It is assumed to form complex three-dimensional polymeric networks (gel-like). An "a priory" estimation of diffusion coefficients is difficult. In general, a log-log linear inverse relationship between first-order desorption rate constants, and the partition coefficients was ob-served (Brusseau et al., 1990). Carroll et al. (1994) applied a permeant/polymer diffusion model to the sorption of polychlorinated biphenyls from river sediments. Freeman and Chang (1981) modeled the desorption of organic compounds from pond sediments using a gel partition model.

Similarly, the uptake of PAHs by aerosol particles was found to be limited by slow diffusive transport through organic phases (Rounds et al., 1993) – the same may apply for microplastics appearing in the environment. Szecsody and Bales (1989) concluded from experiments with different particle and pore sizes, that slow binding and release of 1,4-dichlorobenzene onto phenyl-polymer modified silica is limited by the movement of the solute molecule into and out of the bound organic phase. The diffusion coefficients in the organic matter or organic phase may be significantly lower than in the aqueous phase. Experiments of transport of organic penetrants into bituminous coals showed that the macromolecular structure and the transport properties can depend on the swelling of the organic matter (Barr-Howell et al., 1986). The swelling leads to anomalous diffusion (non-Fickian), which was investigated for diffusion in glassy polymers (Frisch, 1980). Sorptive uptake can be described by a simple power function:

$$\frac{M_s}{M_{eq}} = k_r t^n \tag{4.9}$$

where M_s/M_{eq} is the mass [M] of solute sorbed relative to equilibrium condition (M_{eq}). k_r denotes the empirical relaxation constant, which depends on the structure of the organic polymer and the properties of the penetrant. n is an empirical exponent, which for Fickian diffusion and $M_s / M_{eq} <$ 0.5 is 1/2. For $n > 1/2$, the diffusion process is controlled by the advancement of the boundary between swollen organic matter (or gel) and the non-swollen (glassy) core. Both, Fickian diffusion and relaxation can be coupled. The expression for sorptive uptake from an infinite bath is (Frisch, 1980):

$$\frac{M_s}{M_{eq}} = 1 - X_F \frac{6}{\pi^2} \sum_{n=1}^{\infty} \frac{1}{n^2} \exp\left[-n^2\pi^2 \frac{D_a}{a^2} t\right] - X_R exp[-k_r t] \tag{4.10}$$

where X_F and X_R denote the fraction of equilibrium sorptive uptake due to Fickian diffusion and the contribution from the relaxation process, respectively. a is the radius of the particle [L], and D_a/a^2 is the diffusion rate constant.

The diffusion of organic compounds into synthetic polymers can cause sampling bias. For example, plastic groundwater monitoring well casings can cause organic contaminants to sorb, resulting in underprediction of in-situ aqueous phase concentration in the well (Reynolds et al., 1990). Since synthetic polymers are also used as liners for waste disposal, the diffusive mass transfer of organics across such materials must be taken into account. High diffusion rates have to be expected under steady-state conditions if steep concentration gradients develop in the liner (e.g., for highly sorptive organic compounds).

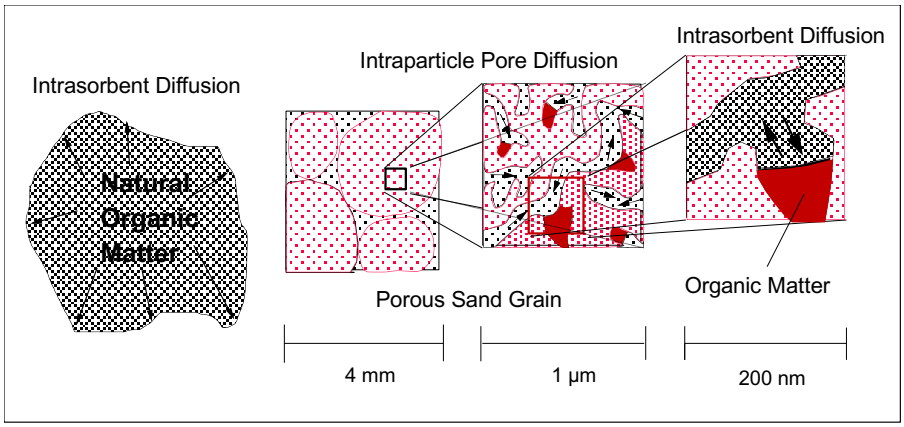

Fig. 4.2: Intra-organic matter (intrasorbent) diffusion, pore and intrasorbent diffusion combined (Mattes, 1993)

4.4 VAPOR PHASE DIFFUSION IN THE VADOSE ZONE

Under natural conditions, only minor pressure gradients exist in the subsurface environment (according to Jury et al., 1991 only 0.5%, 1%, 0.1%, and 7% - 8% of the overall gas exchange are caused by temperature effects, barometric pressure changes, wind, and precipitation, respectively). Therefore, the mass transfer of gaseous compounds in the unsaturated soil zone is generally governed by vapor phase diffusion.

Since the diffusion coefficients in a gas are much higher than in a liquid (by a factor of 10 000), the diffusive flux in the unsaturated zone depends mainly on the air-filled pore space, which is a function of the water content. Similar to the definition of the diffusion coefficients in the water-saturated zone, the effective gas diffusion coefficient (D_{eg}) in the unsaturated water zone can be calculated based on empirical correlations of the general form (Currie, 1960):

$$\frac{D_{eg}}{D_g} = \frac{n_g}{\tau_f} = f(n_g) \approx b \cdot n_g^m \tag{4.11}$$

where D_g, $D_{eg,}$ and n_g are the molecular gas diffusion coefficient, the effective diffusion coefficient in the vadose zone, and the air-filled porosity, respectively. b and m are empirical constants. Millington and Quirk (1960) proposed to include additionally the overall porosity (n). Sallam et al. (1984) extended these correlations to low air-filled porosities (4-12a):

$$\frac{D_{eg}}{D_g} = \frac{n_g^{3.1}}{n^2} \tag{4.12a}$$

A new relationship was developed by Moldrup et al. (2000), which gave good predictions for sandy materials (see Wang et al., 2003):

$$\frac{D_{eg}}{D_g} = \frac{n_g^{2.5}}{n} \tag{4.12b}$$

Fig. 4.3 shows a comparison of some selected empirical correlations and Table 4.1 gives some examples for D_{eg}.

Under transient conditions, the capacity factor is used for the calculation of the apparent diffusion coefficient (D_{ag}) in the vadose zone:

$$D_{ag} = \frac{D_{eg}}{\alpha};\ \alpha = n_g + \frac{n_w}{H} + \frac{K_d \rho}{H} = (n - w\rho) + \frac{w\rho}{H} + \frac{K_d \rho}{H} \tag{4.13}$$

Here n denotes the porosity, while before we use ε. The reason for this is that two porosities may occur in parallel: inter- and intragranular porosities. The first one (n) allows also fast transport (of water or air) while the latter (ε) is restricted to diffusion in pore water.

Table 4.1: Calculated diffusion coefficients in sand, silt, and clay under natural conditions (e.g., typical water contents and porosities) according to the correlation reported by Sallam et al., 1984.

				Sand	*Silt*	*Clay*
			porosity:	*n*	0.4	0.48	0.54
			air filled porosity:	n_g	0.36	0.12	0.027
			diffusion coefficient [$cm^2 s^{-1}$]:	D_g	D_{eg}	D_{eg}	D_{eg}
O_2	32	11	0.22	0.057	13×10^{-4}	10×10^{-6}
CO_2	44	27.5	0.15	0.040	9.2×10^{-4}	7.1×10^{-6}
CH_4	16	24.5	0.20	0.054	12×10^{-4}	9.6×10^{-6}
Benzene	78	90.8	0.087	0.023	0.53×10^{-4}	4.1×10^{-6}

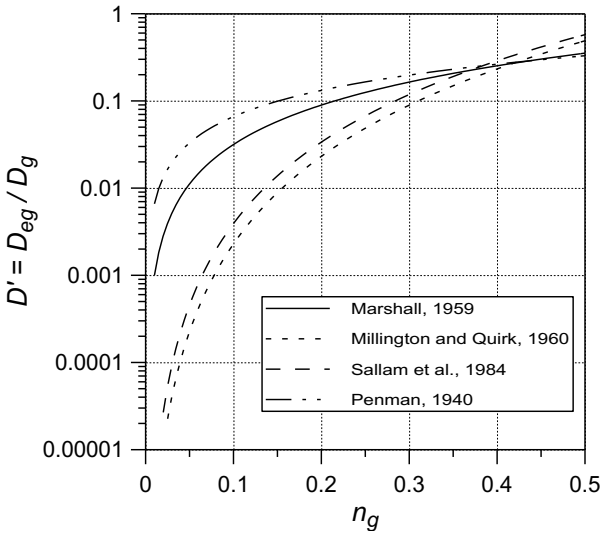

Fig. 4.3: Diffusivities in the vadose zone *vs.* the air-filled porosity.

4.5 SOME REMARKS CONCERNING THE CALCULATION OF DIFFUSION COEFFICIENTS

The measurement of diffusion coefficients is time-consuming and requires sophisticated experimental procedures. Therefore, empirical models are frequently used to assess diffusive solute transport through a porous sample (e.g., clays and sedimentary rocks). Effective diffusion coefficients for steady-state conditions can be predicted reasonably well from the porosity based on Archie's law using an empirical exponent of 2.2 (between 1.8 and 2.4, Boving and Grathwohl, 2001):

$$D_e = D_{aq}\varepsilon^{2.2} \tag{4.14}$$

This may also be applied to predict pore diffusion coefficients in homogeneous, low organic carbon content particles, especially coarse sand and gravel (e.g., carbonate lithocomponents). The pore diffusion coefficient is:

$$D_p = D_{aq}\varepsilon^{2.2-1} \tag{4.15}$$

The prediction of the apparent diffusion coefficient requires the sorption coefficients of various compounds. The sorption coefficients (e.g., K_d) can be estimated based on the organic carbon content (oc [mg/g]) and the organic carbon-based sorption coefficient K_{oc} (for the prediction of K_{oc} see Sections on Sorption: K_{ow} - K_{oc} - Solubility relationships):

$$K_d = K_{oc}\frac{oc}{1000} \tag{4.16}$$

Extension of Eq. 6.1 by a "sorption" capacity term yields:

$$D_a = \frac{D_{aq}\varepsilon^{2.2-1}}{1 + K_{oc}\frac{oc}{1000}\frac{\rho}{\varepsilon}} \tag{4.17}$$

Table 4.2 shows a summary of values of D_a to be expected in natural porous media. The properties of the porous media were chosen roughly according to frequently occurring values.

Table 4.2: Apparent diffusion coefficients (D_a [cm²/s]) for some organic pollutants estimated for sedimentary rocks and clay/silt layers (Archie's law exponent: m =2.2)

				Carbonates	Mudstone	Sandstone	Clay	Silt
			ε [-]	0.03	0.15	0.1	0.35	0.35
			oc [mg/g]	0.10	0.50	0.05	0.50	0
	log K_{ow}	log K_{oc}	D_{aq}	D_a	D_a	D_a	D_a	D_a
Tracer (Iodide)	-	-	1.9E-05	2.5E-07	1.8E-06	1.2E-06	5.2E-06	5.3E-06
Trichloroethene	2.42	2.01	8.4E-06	1.3E-08	9.9E-08	2.4E-07	6.8E-07	2.4E-06
Toluene	2.69	2.24	8.0E-06	7.5E-09	5.8E-08	1.6E-07	4.3E-07	2.3E-06
Naphthalene	3.36	2.78	7.0E-06	2.0E-09	1.6E-08	5.4E-08	1.3E-07	2.0E-06
Phenanthrene	4.57	3.76	5.9E-06	1.8E-10	1.4E-09	5.4E-09	1.2E-08	1.7E-06
Pentachlorophenol	5.01	4.11	4.7E-06	6.3E-11	5.0E-10	1.9E-09	4.2E-09	1.3E-06
Benzo(a)pyrene	6.50	5.31	4.9E-06	4.2E-12	3.3E-11	1.3E-10	2.8E-10	1.4E-06

This simple procedure for predicting diffusion parameters has limitations in the cases of sorption/desorption kinetics in heterogeneous samples (e.g. mixtures of rock fragments or particulate organic matter in granular media). If a single component diffusion model is used to determine the diffusion rate constants from sorptive uptake and desorption data, then diffusion parameters such as effective diffusivities and tortuosity factors would be affected. Overall, K_d and intraparticle porosities determined for the bulk samples are not useful in calculating tortuosity factors - the resulting values would be too high if only a small fraction of the sample causes a large fraction of the sorptive uptake (as often is the case). Sorption/desorption kinetics monitored over a limited period in a mixed sand sample with solutes of different sorptivity (different pore retardation) would be representative of different components of the sample. A fraction of "instantaneous or fast sorption" would decrease with increasing sorptivity of the compounds. In such cases, tortuosities would show an apparent dependency on the sorptivity (K_{ow}) of the compounds. This may be considered as an artifact arising from the modeling of a heterogeneous sample with a one-component homogeneous model (see later chapters about sorption kinetics).

In humic soil samples and peat, slow sorptive uptake and desorption of organic compounds may be due to diffusion in organic matter (intrasorbent diffusion). Particles could contain organic matter as pore fillings. If the time necessary for diffusion into the particle approaches the time needed for diffusion into organic matter filled pores, then the particle radius no longer represents the effective diffusion distance. In such cases, tortuosity factors, which are calculated based on the particle radius, would increase with decreasing grain size, which was observed for some sand samples.

In steady-state diffusion of organic compounds through a porous medium, organic matter filled pores do not contribute to the diffusive flux if the organic matter has a low degree of connectivity. If the solid surface is coated with organic matter or pore conduits are filled with organic matter, a significant contribution to the steady flux is possible. This even applies when diffusion coefficients in organic matter are lower than in the aqueous phase. This is due to the sorption of the organic compounds in the organic matter resulting in high concentration gradients.

In clays with high surface areas or significant amounts of expandable clay minerals, the overall porosity does not represent the transport-through porosity (diffusion-effective porosity). Adding organic sorbents such as coal and bituminous shales to mineral liners delays the breakthrough of organic contaminants considerably. However, the retardation factors for contaminants diffusing through the liner materials may be lower than those expected from equilibrium sorption

isotherms of the additives. This indicates that either sorption is not at equilibrium or preferential diffusion in such samples may occur.

In summary, the prediction of diffusion parameters from independently measured properties of the porous media (e.g., *oc*, ε) is certainly possible for sedimentary rock such as limestones, sandstones, and mudstones, as well as for silt and non-swelling clay layers. In heterogeneous sand or gravel aquifer materials, predicting the intraparticle diffusion parameters is only possible for a specific lithocomponent (or a multicomponent model is used). From a practical point of view, this component should be selected based on the time scale of interest (e.g., large particles with high sorption capacity for predicting long-term sorption/desorption behavior of contaminants and vice versa).

5. DIFFUSION IN LAYERS OF LOW PERMEABILITY

Diffusion often is the dominant mass transfer mechanism (compared to advection) in zones of low hydraulic conductivity such as clay and silt layers, lenses, fractured rock matrixes (matrix diffusion). In technical seals such as mineral liners at landfills or slurry walls, contaminant transport predominantly takes place by diffusion. The geometry of these layers may be considered as plane sheets, and analytical solutions of Fick's 2nd law are available for a variety of initial and boundary conditions (Crank, 1975).

5.1 DIFFUSION INTO AND OUT OF SEMI-INFINITE POROUS MEDIA

Thick confining layers and bedrock formations of low permeability may represent a sink for contaminants that are spread out in an aquifer or a landfill. Once such low-permeability domains are contaminated, they may become a long-term source during remediation of the aquifer (e.g., pump-and-treat). These formations can be considered as semi-infinite porous media. If the low conductivity zone is free of the contaminant initially and then exposed to a constant concentration at the surface for a given period, following initial and boundary conditions apply:

$t = 0 \quad x > 0 \quad C = 0$

$t > 0 \quad x = 0 \quad C = C_0$

$t > 0 \quad x = \infty \quad C = 0$

The concentration profile at a given time within the low conductivity zone is:

$$\frac{C}{C_0} = \operatorname{erfc}\left[\frac{x}{2\sqrt{D_a t}}\right] \tag{5.1}$$

where "erfc" denotes the complementary error function, which is further explained in Box 5.1. The quantity $\sqrt{D_a t}$ can be considered as "penetration depth," which represents the time-dependent distance within which 87% of the mass of the diffusing substance occurs. Accordingly, the "penetration time" then represents the time after which 87% of the diffusing molecules have not yet moved beyond a given distance. Fig. 5.1 shows concentration distributions for different values of $D_a t$. Box 5.2 compares solutions for the infinite and semi-infinite case.

The mass of solute per unit area which has diffused into the low conductivity zone after a certain time is:

$$\mathrm{M} = 2C_0\alpha\sqrt{\frac{D_a t}{\pi}} \quad [ML^{-2}] \tag{5.2}$$

The flux per unit area at the interface at time t is given by the time derivative of Eq. 5-2:

$$\mathrm{F} = C_0\alpha\sqrt{\frac{D_a}{\pi t}} \quad [ML^{-2}t^{-1}] \tag{5.3}$$

In the case of a nonsorbing solute, the capacity factor α equals the porosity of the confining layer. Since α also occurs in the denominator of D_a, the uptake rates increase with the square root of α. Eqs. 5.2 and 5.3 are equivalent to the short-term approximations of the finite cases (e.g., for diffusion in particles of various shape) provided that the appropriate expressions for M_{eq} (see Eq. 5.3) are applied.

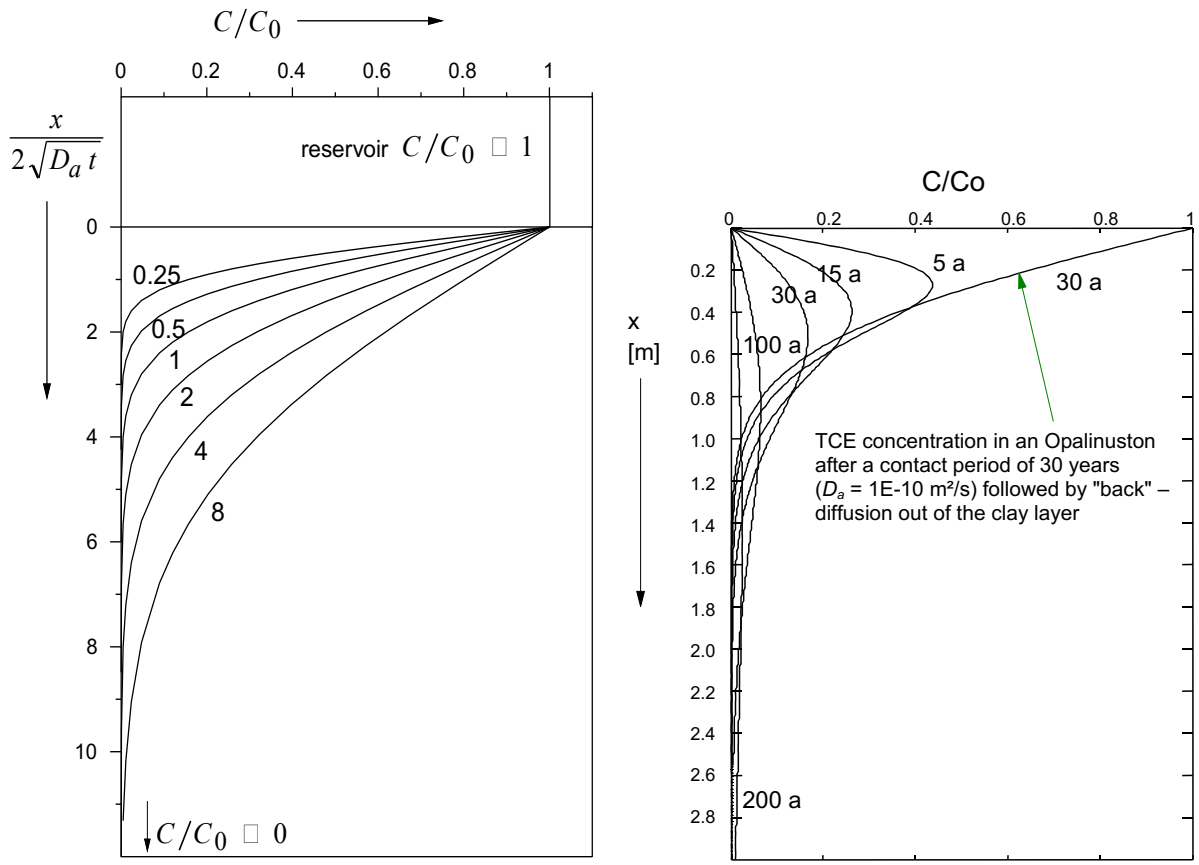

Fig. 5.1: Left - diffusion from a reservoir of constant concentration into a semi-infinite medium (e.g., a confining layer). Numbers represent different times expressed as $D_a\,t$. Right – diffusion into and out of a semi-infinite porous medium (backdiffusion).

If after a certain time of exposure (t_e), the concentration at the surface (C_0) is decreased to zero (e.g., because of remedial actions), then one fraction of the solute will start to diffuse out of the low conductivity zone and the rest will still diffuse further into the confining layer (see Fig. 5.1, right). The initial and boundary condition for this case may be expressed as:

$t = 0 \quad x > 0 \quad C/C_0 = \mathrm{erfc}[x/(4D_a t_e)^{0.5}]$

$t > 0 \quad x = 0 \quad C = 0$

$t > 0 \quad x = \infty \quad C = 0$

The diffusive flux out of the low conductivity zone then is given by:

$$\mathrm{F} = C_0\,\alpha\sqrt{\frac{D_a}{\pi t}}\left(1-\frac{1}{\sqrt{1+t_e/t}}\right) \quad [ML^{-2}t^{-1}] \tag{5.4}$$

The mass of solute which has left the confining layer after a given time is:

$$M = 2\,C_0\,\alpha\sqrt{\frac{D_a\,t}{\pi}}\left(1-\sqrt{1+t_e/t}+\sqrt{t_e/t}\right) \quad [ML^{-2}] \tag{5.5}$$

Similar solutions are given by Bear et al. (1994).

Eq. 5.5 may also be expressed as the mass relative to the mass present in the porous media at t = 0 ("desorption time"), which is the mass of solute after exposure for a given time t_e ("sorption time": M_{te} is given by Eq. 5-2 with $t = t_e$):

$$\frac{M}{M_{te}} = 1 - \left(\sqrt{1 + t/t_e} - \sqrt{t/t_e}\right)$$

and for $t >> t_e$: (5.6)

$$\frac{M}{M_{te}} = 1 - \left(\sqrt{t_e/4t}\right)$$

The fluxes are easily obtained from Eq. 5.6 by the time derivative, and for $t >> t_e$, they decrease with a slope of -3/2 in a double-logarithmic plot of F versus time:

$$\frac{F}{M_{te}} = \frac{1}{4}\sqrt{\frac{t_e}{t^3}} \tag{5.7}$$

This $t^{3/2}$ law, for example, was observed in reactive tracer experiments on radionuclides transport in fractured rocks at the Grimsel test site in Switzerland (Heer and Haderman, 1994).

Eq. 5.7 is again equivalent to the short-term approximation for diffusion into a sphere, provided that M_{te} is expressed in terms of M_{eq} which is $M_{te} = 6\ M_{eq} / a\ (D_a\, t_e / \pi)^{0.5}$. Fig. 5.2 shows cumulative masses and fluxes into and out of a semi-infinite medium.

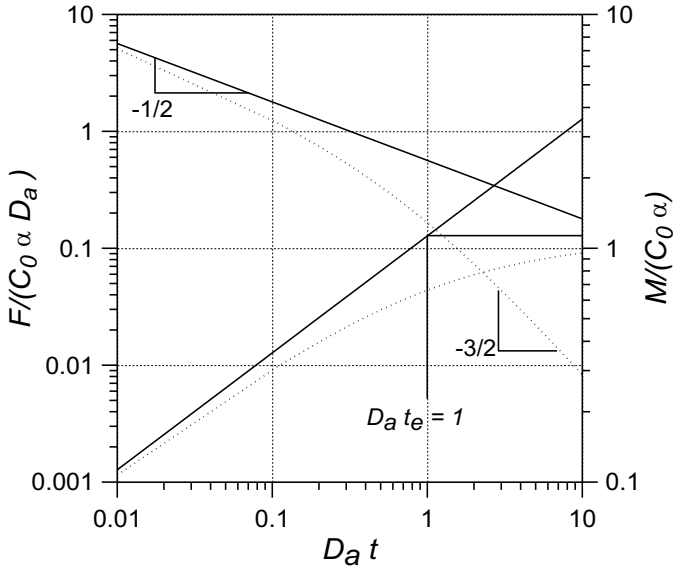

Fig. 5.2: Flux (descending lines) and cumulative mass (ascending lines) into (solid lines) and out of a semi-infinite medium after $\boldsymbol{D_a t_e = 1}$ (dotted lines).

Box 5.1: The complementary error function (erfc)

Definition:

$\mathrm{erfc}(\beta) = 1 - \mathrm{erf}(\beta)$

solid line: erfc

dotted line: erf

dashed line: derivative of erf

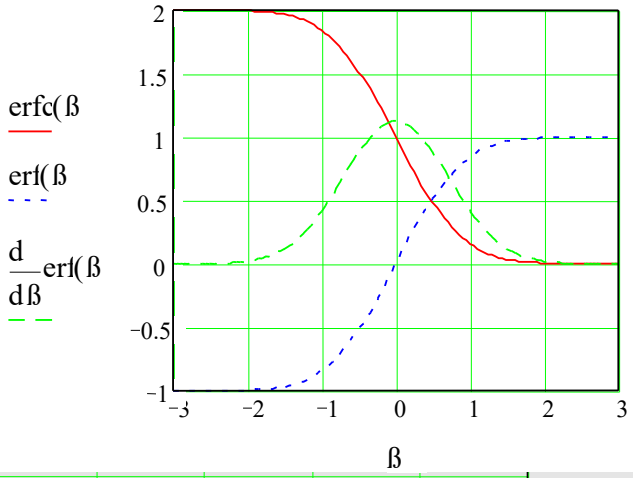

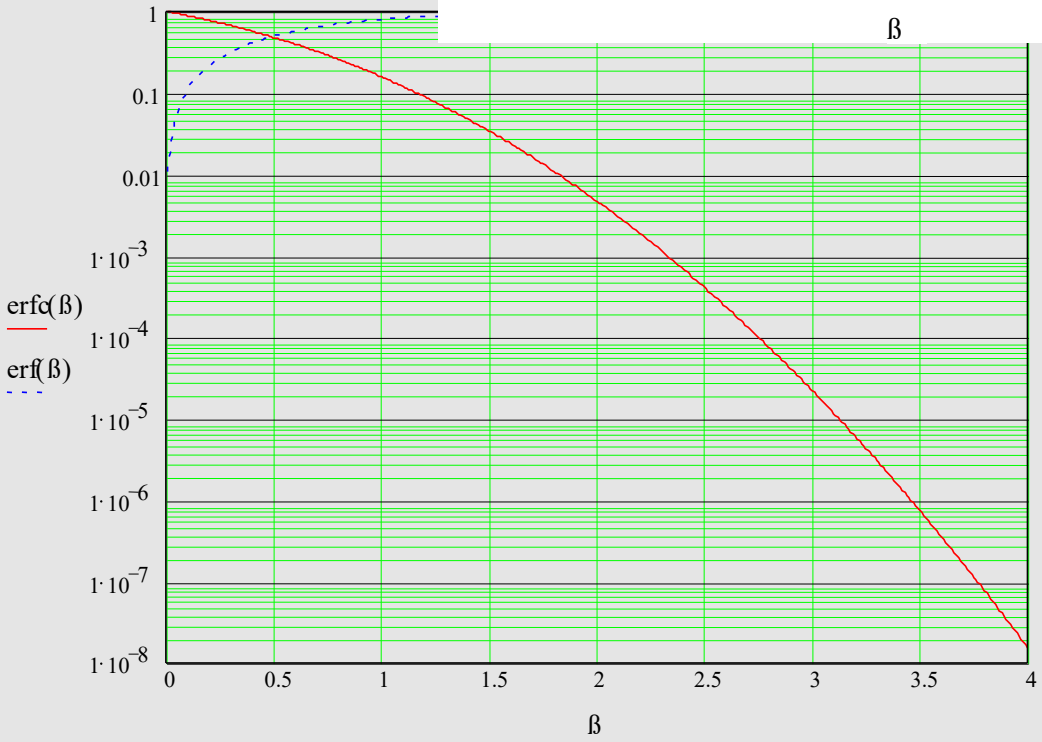

Box 5.2: Solutions of Fick's 2nd Law in for infinite boundary conditions

Infinite case, inital condition: $C = 0$, $t = 0$, $x > 0$; $C = C_o$, $t = 0$, $x < 0$;
Boundary condition: $C = 0$, $t > 0$, $x = +\infty$; $C = C_o$, $t > 0$, $x = -\infty$ (continuous source)

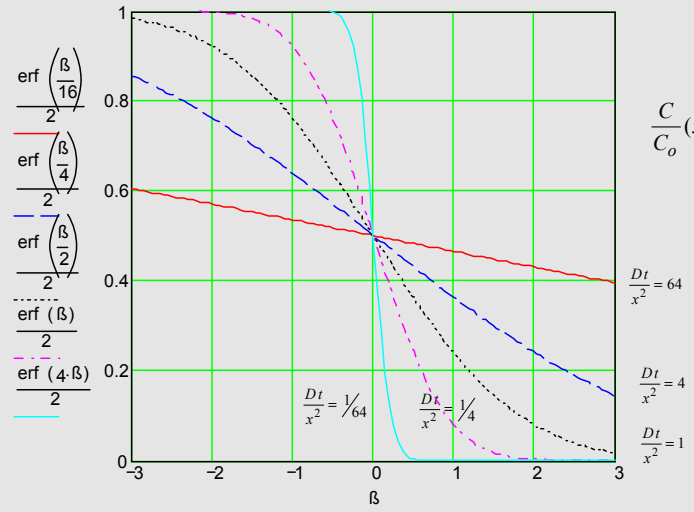

$$\frac{\partial C}{\partial t} = D\frac{\partial^2 C}{\partial x^2}$$

$$\frac{C}{C_o}(x,t) = 0.5\ \mathrm{erfc}\left(\frac{x}{\sqrt{4Dt}}\right)$$

$$\beta = \frac{x}{\sqrt{4Dt}}$$

Semi-infinite case, initial condition: $C = 0$, $t = 0$, $x \geq 0$;
Boundary condition: $C = C_o$, $t > 0$, x = 0; $C = 0$, $t > 0$, $x = \infty$

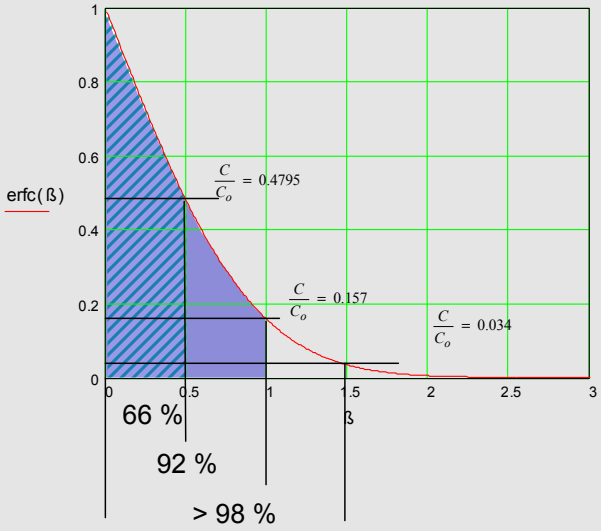

$$\frac{\partial C}{\partial t} = D\frac{\partial^2 C}{\partial x^2}$$

$$\frac{C}{C_o}(x,t) = \mathrm{erfc}\left(\frac{x}{\sqrt{4Dt}}\right)$$

$$\beta = \frac{x}{\sqrt{4Dt}}$$

$$x = \beta\sqrt{4Dt}$$

5.2 DIFFUSION ACROSS CONFINING LAYERS

Solute diffusion across a confining layer is relevant especially for mineral liners or other seals at waste disposal sites such as slurry walls for vertical containment of contaminants. The initial and boundary conditions for a confining layer of thickness d [L], which is initially free of solute, and the concentration at $x = d$ is kept constant (e.g. close to 0), while the diffusion takes place from a reservoir of constant concentration (C_0) are:

$t = 0 \quad x > 0 \quad C = 0$

$t > 0 \quad x = 0 \quad C = C_0$

$t > 0 \quad x = d \quad C = 0$

The concentration profile at time t in the layer is given by:

$$\frac{C}{C_0} = 1 - \frac{x}{d} - \frac{2}{\pi}\sum_{n=1}^{\infty}\frac{1}{n}\sin\left[\frac{n\pi x}{d}\right] exp\left[\frac{-n^2\pi^2 D_a t}{d^2}\right] \tag{5.8}$$

Fig. 5.3 shows the concentration profiles of a diffusing solute at different times. After a certain time, when steady-state conditions are reached, the concentration profile becomes a straight line.

The analytical solution for the contaminant mass which has diffused through the liner per unit area (e.g., left the liner at $x = d$) is given by:

$$M = C_0\,\alpha\,d\left(\frac{D_a t}{d^2} - \frac{1}{6} - \frac{2}{\pi^2}\sum_{n=1}^{\infty}\frac{(-1)^n}{n^2} exp\left[\frac{-n^2\pi^2 D_a t}{d^2}\right]\right) \tag{5.9}$$

For long periods the series expansion in Eqs. 5.8 and 5.9 vanishes, and a linear relationship is obtained between M and t, (and between C/C_0 and x => steady-state conditions):

$$\begin{aligned} M &= C_0\,\alpha\,d\left(\frac{D_a t}{d^2} - \frac{1}{6}\right) \\ &= C_0\left(D_e\frac{t}{d} - \frac{\alpha d}{6}\right) \end{aligned} \tag{5.10}$$

The steady-state flux is obtained easily by the time derivative of Eq. 5.10:

$$F_{stat} = D_e\frac{C_0}{d} \tag{5.11}$$

which corresponds to Fick's 1st law. The intercept of Eq. 5.10 with the time axis is commonly denoted as lag-time (t_{lag}):

$$t_{lag} = \frac{d^2\alpha}{6\,D_e} = \frac{d^2}{6\,D_a} \tag{5.12}$$

t_{lag} is approximately 1/3 of the time necessary to reach steady-state conditions.

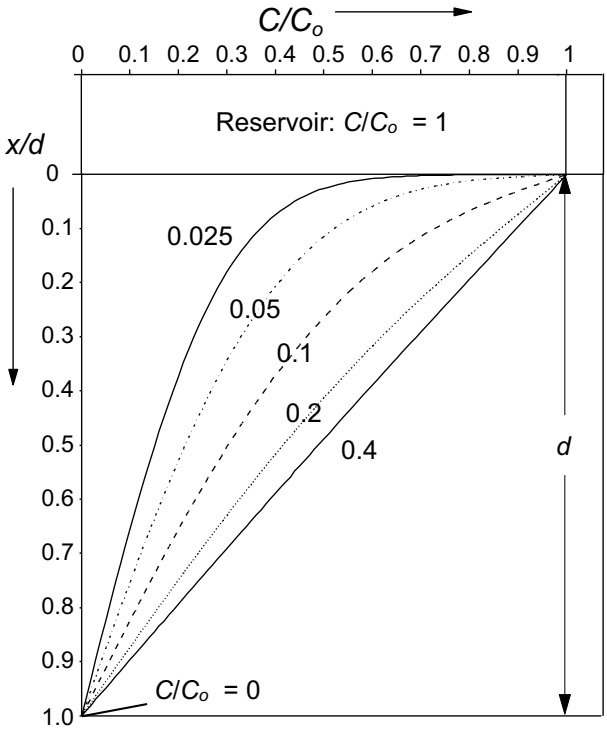

Fig. 5.3: Diffusion from a reservoir of constant concentration into a layer of thickness *d*. The numbers represent dimensionless time expressed as $D_a\, t/d^2$.

As outlined above, the contaminant diffusion through liners, or confining layers in general, is essentially characterized by the steady-state flux (Eq. 5.11) and t_{lag}. F_{stat} depends linearly on the thickness of the liner ($1/d$) and the effective diffusion coefficient. The time to reach steady-state conditions increases linearly with increasing capacity factor ($\alpha = \varepsilon + K_d\rho$) but with the square of the thickness of the layer (d^2).

The pre-steady-state flux leaving the liner at $x = d$ is (Thoma et al., 1993):

$$F = \left(C_0 \alpha \frac{D_a}{d}\right)\left(1 + 2\sum_{n=1}^{\infty}(-1)^n \exp\left[\frac{-n^2\pi^2 D_a t}{d^2}\right]\right) \tag{5.13}$$

Since the first term here represents the steady-state flux (Eq. 5.10), normalization of Eq. 5.13 yields (Wang et al., 1991):

$$\frac{F}{F_{stat}} = 1 + 2\sum_{n=1}^{\infty}(-1)^n \exp\left[\frac{-n^2\pi^2 D_a t}{d^2}\right] \tag{5.14}$$

which has the following short-term approximation (Crank, 1975):

$$\frac{F}{F_{stat}} = 2\sqrt{\frac{d^2}{\pi D_a t}}\, \exp\left[\frac{-d^2}{4D_a t}\right] \tag{5.15}$$

Fig. 5.4 shows the cumulative mass diffused through the liner and F/F_{stat} compared to the long-term and short-term approximations. At $t = t_{lag}$ ($D_a\, t/d^2 = 1/6$), 61.67 % of the steady-state flux through the liner is reached (for analytical solutions for different boundary conditions and a two-layer system, see Thoma et al., 1993).

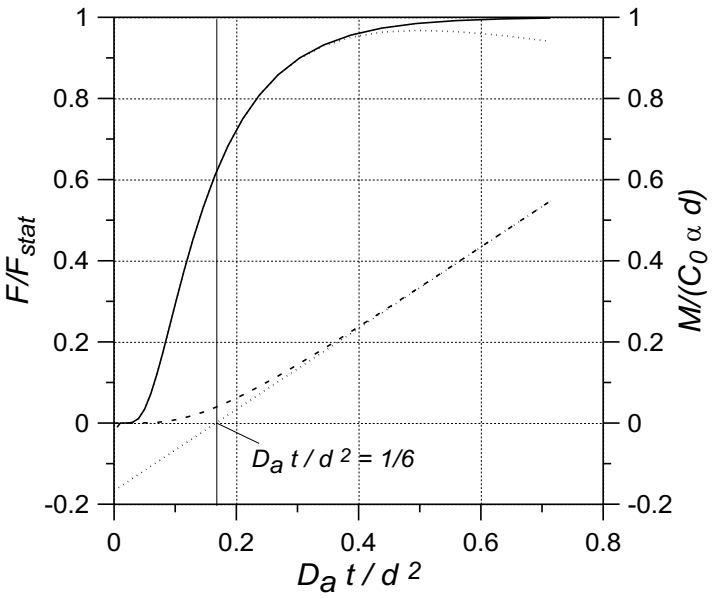

Fig. 5.4: Normalized flux (solid line, Eq. 5.13) with short-term approximation (dotted line, Eq. 5.15) and normalized cumulative mass (dashed line, Eq. 5.9) with long-term approximation (dotted line, Eq. 5.10) for diffusion through a layer.

6. DIFFUSION - REACTION: WEATHERING FRONT

A illustrating example for propagation of concentration fronts is the weathering of rocks which involves the oxidation of organic matter or mineral phases such as Fe^{2+} - bearing species (pyrite, siderite, saddle dolomites). Oxygen diffuses from the atmosphere into the porous medium and a reaction front develops as shown in Fig. 6.1 (see e.g., Lebedeva et al., 2007; Bao et al., 2018).

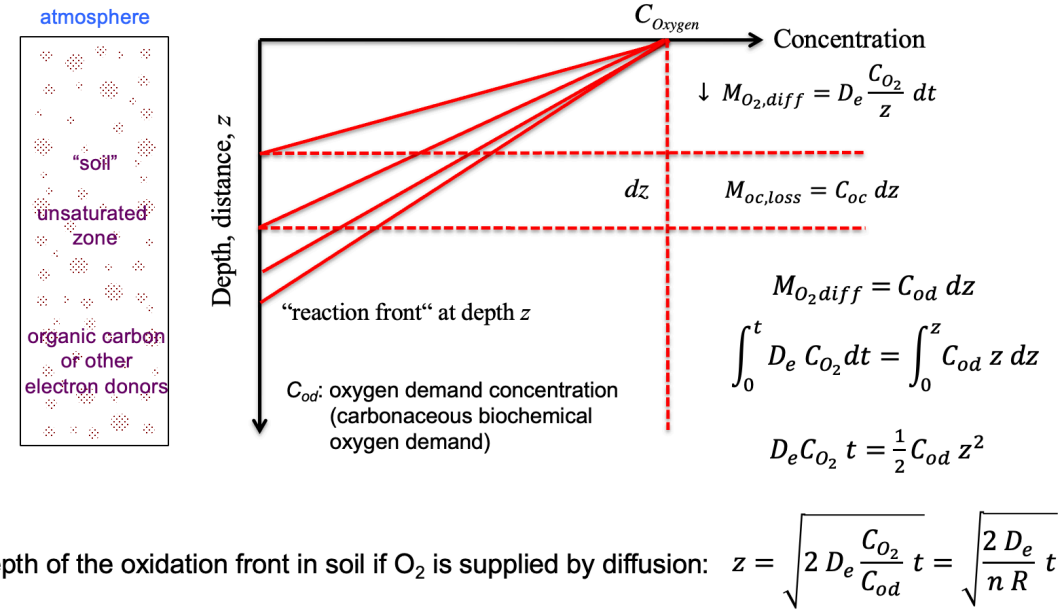

Fig. 6.1: Progress of a weathering front e.g., during oxidation of organic carbon (oc) with a fixed O_2 concentration at the surface; $M_{O2,diff}$, $M_{oc,loss}$: O_2 (electron acceptor) mass diffused from the atmosphere into the porous media and organic carbon lost (electron donor), D_e, C_{O2}, C_{oc}: effective diffusion coefficient, concentrations of O_2 and oc; C_{od} denotes the oxygen demand (an analogous approach may be used to calculate the progress of an oxidation front e.g. if Fe^{2+} bearing minerals are present).

The depth of the weathering (oxidation) front (z) may be based on mass balance considerations (see also Fig. 6.1):

$$\int_0^t D_e\, C_{O_2} dt = \int_0^z C_{od}\, z\, dz$$
$$D_e\, C_{O_2}\, t = \frac{1}{2} C_{od}\, z^2 \qquad (6.1)$$
$$z = \sqrt{2\, D_e \frac{C_{O_2}}{C_{od}}\, t} = \sqrt{\frac{2\, D_p}{R}\, t}$$

C_{od} denotes the oxygen demand as explained in Box 6.1. R is a retardation factor ($R = C_{od}/(n\, C_{O2})$; D_p is the pore diffusion coefficient (D_e/n) and D_p/R is the apparent diffusion coefficient.

Box 6.1: Example for a "reactive" weathering front

The oxygen demand during oxidation of organic carbon depends on the stoichiometry of the reaction, e.g.: 1 mol carbon needs 1 mol O_2 for oxidation (yielding one CO_2 molecule for each C atom), thus 12 grams of carbon consume 32 grams of oxygen or 2.67 g of oxygen are needed to oxidize 1 gram of oc. The stoichiometric coefficient γ here is mass based (= 2.67). This leads to the oxygen demand (C_{od}) which may be considered as the oxygen consumption capacity per unit volume porous medium (also including the initially O_2 free pore space: $C_{od} = \gamma_m\, f_{oc}\, \rho_{bulk} + C_{oxygen}\, n$).

Example: Weathering of a jurassic mudstone (e.g. Opalinuston) causes depletion of organic carbon (and oxidation of pyrite). Weathering results in a almost water saturated clay (with a color change from dark grey to ocher because of production iron hydroxides, e.g. goethite) with a porosity close to 50%. Aqueous diffusion coefficients (D_{aq}) are in the order of 1 x 10^{-9} m^2 s^{-1} and $D_e \approx D_{aq}\, n^2$; $D_p \approx D_{aq}\, n$.

The aqueous oxygen concentration in recharge water in equilibrium with the atmosphere is 10 g/m^3 (C_{oxygen}). If we neglect pyrite oxidation and assume an organic carbon content of 1 weight % to be oxidized, the depth of the oxidation front after time t (e.g. 10000 years after the last ice age) may be calculated:

$$z = \sqrt{2\frac{D_e\, C_{oyxgen}}{C_{od}}\, t} = \sqrt{2\frac{D_{aq}\, n^2\, C_{oyxgen}}{\gamma\, f_{oc}\, \rho_{bulk} + n\, C_{oxygen}}\, t} \quad \left(= \sqrt{2\frac{D_p}{\frac{\gamma\, f_{oc}\, \rho_{bulk}}{n\, C_{oyxgen}} + 1}\, t} = \sqrt{2\frac{D_p}{R}\, t} \right)$$

$$= \sqrt{2\frac{1\times10^{-9}\ \mathrm{m^2\ s^{-1}} \times 0.5}{\frac{2.67 \times 0.01 \times (1-0.5) \times 2700\ \mathrm{kg/m^3}}{0.01\ \mathrm{kg/m^3} \times 0.5} + 1} \times 10000\ \mathrm{a}} = \sqrt{\frac{158\ \mathrm{m^2}}{\frac{36}{0.005} + 1}} = \sqrt{\frac{158\ \mathrm{m^2}}{7201}} = 0.15\ \mathrm{m}$$

The depth of the rection front is quite short and thus the question comes up how deep it would be if water infiltration (groundwater recharge) is considered. The retardation factor in that case is the same as in the pure diffusion case:

$$R = \frac{C_{od}}{n\, C_{oxygen}} = \frac{\gamma\, f_{oc}\, \rho_{bulk} + n\, C_{oxygen}}{n\, C_{oyxgen}} = \frac{\gamma\, f_{oc}\, \rho_{bulk}}{n\, C_{oyxgen}} + 1 = \frac{2.67 \times 0.01 \times 1350\ \mathrm{kg/m^3}}{0.005\ \mathrm{kg/m^3}} + 1 = 7210$$

For a groundwater recharge rate (q) of 0.5 mm d^{-1} (=0.1825 m a^{-1}) we get:

$$z = \frac{q\, t}{n\, R} = \frac{0.1825}{0.5 \times 7210} \times 10000 = 0.5\ \mathrm{m}$$

Thus, groundwater recharge dominates the progress of weathering fronts in the long term.

7. TRANSPORT BY DIFFUSION OVERTAKEN BY ADVECTION

In unconsolidated sand and gravel aquifers, contaminant transport is primarily due to the advection of the groundwater. During soils-air-venting for remediation of volatile organic compounds in the unsaturated zone advection is also the dominant transport mechanism. In zones of low conductivity (e.g., rock matrix, shales, clay, and silt formations), advection is very slow due to the low hydraulic conductivities and aqueous diffusion is considered the predominant migration mechanism of contaminants. Whether this assumption is correct depends on scale in time and space. E.g., the velocity of diffusive migration of a solute from a source of constant concentration into a semi-infinite medium may be derived from the argument (β) of the complementary error function (erfc; see Boxes 5.1 - 5.2) which is:

$$\beta = \frac{x}{2\sqrt{D_a t}} \tag{7.1}$$

For β = 0.5, the complementary error function yields a value of 0.4795. This means that the distance x traveled by a contaminant front with a relative concentration of approximately 0.5 (exactly C/C_o = 0.4795) after time t is:

$$x = \sqrt{D_a t} = \sqrt{\frac{D_e}{\varepsilon\, R_d} t} \tag{7.2}$$

The diffusion velocity (v_d) or propagation of a given solute concentration decreases with the square root of time, for $C/C_o \cong 0.5$:

$$v_{d(0.5)} = \frac{x}{t} = \sqrt{\frac{D_a}{t}} \tag{7.3}$$

According to Darcy's law, the velocity of purely advective migration of contaminants depends on the hydraulic conductivity (k_f), the hydraulic gradient (i), the (effective) porosity (ε), and the retardation factor ($R=1+K_d\,\rho/\varepsilon$):

$$v_r = \frac{x}{t} = \frac{k_f i}{\varepsilon\, R} \tag{7.4}$$

where v_r denotes the retarded velocity [L t^{-1}] of the contaminant. In contrast to the diffusive migration, the distance traveled by advection is proportional to t, meaning that the initial diffusion dominated migration ultimately becomes dominated by an advective component (Fig. 7.1). From the considerations discussed above, a critical time (t_c) or a corresponding distance (x_c), representing the upper limit of diffusion dominated transport, may be defined:

$$t_c = D_a \left(\frac{\varepsilon\, R}{k_f i}\right)^2 = D_e \frac{\varepsilon\, R}{\left(k_f i\right)^2}$$
$$x_c = \frac{D_a\, \varepsilon R}{k_f i} = \frac{D_e}{k_f i} \tag{7.5}$$

Note, the same porosities ε are used for diffusion and transport, but depending on the porous media different effective porosities have to be used for diffusion, advection and storage (see Box 7.1). For sorbing compounds it takes R times longer to reach x_c compared to a non-reactive tracer. Close to x_c and t_c the solute migration due to the combination of advection and dispersion has to

be considered. This can be calculated using the analytical solution of the advection-dispersion model (ADM) (Ogata and Banks, 1961):

$$\frac{C}{C_0} = 0.5\left[\operatorname{erfc}\left(\frac{x - v_r t}{2\sqrt{D_l\, t}}\right) + \exp\left(\frac{x\, v_r}{D_l}\right)\operatorname{erfc}\left(\frac{x + v_r\, t}{2\sqrt{D_l\, t}}\right)\right] \tag{7.6}$$

where v_r and D_l denote the retarded average linear velocity of the solute front and the longitudinal dispersion coefficient, respectively. At very low flow velocities, mechanical dispersion can be neglected, and D_l approaches D_a.

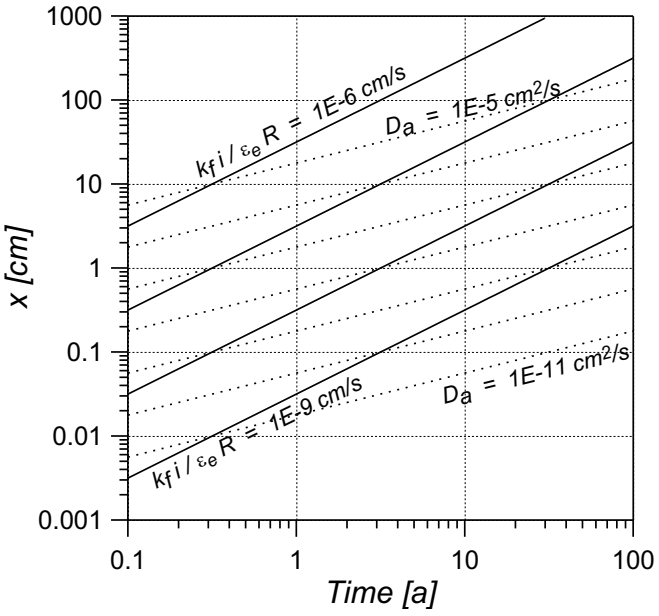

Fig. 7.1: Solute migration due to advection (solid lines) compared to diffusion (dashed lines) calculated for movement of C/C_0 = 0.5 and 0.4795, respectively.

Fig. 7.2 compares concentration profiles for pure diffusion and advection for transport into a semi-infinite porous medium of low conductivity (for pure diffusion: v_r = 0 and $D_l = D_a$; Eq. 7.6 then equals Eq. 5.1; for the pure advection case minimum dispersion was used: $D_l << D_a$). For short periods (in this example, about 10 years), pure diffusion yields almost identical results for the concentration profiles as the advective/diffusive (dispersive) transport does. For more extended time periods, advective/diffusive transport is faster than diffusion alone. Finally, Fig. 7.3 shows the increase of the solute concentrations at a given distance (0.1 m). Again, the breakthrough curves overlap for the periods smaller than 10 years. After 10 years, they diverge due to the effect of the additional advective transport.

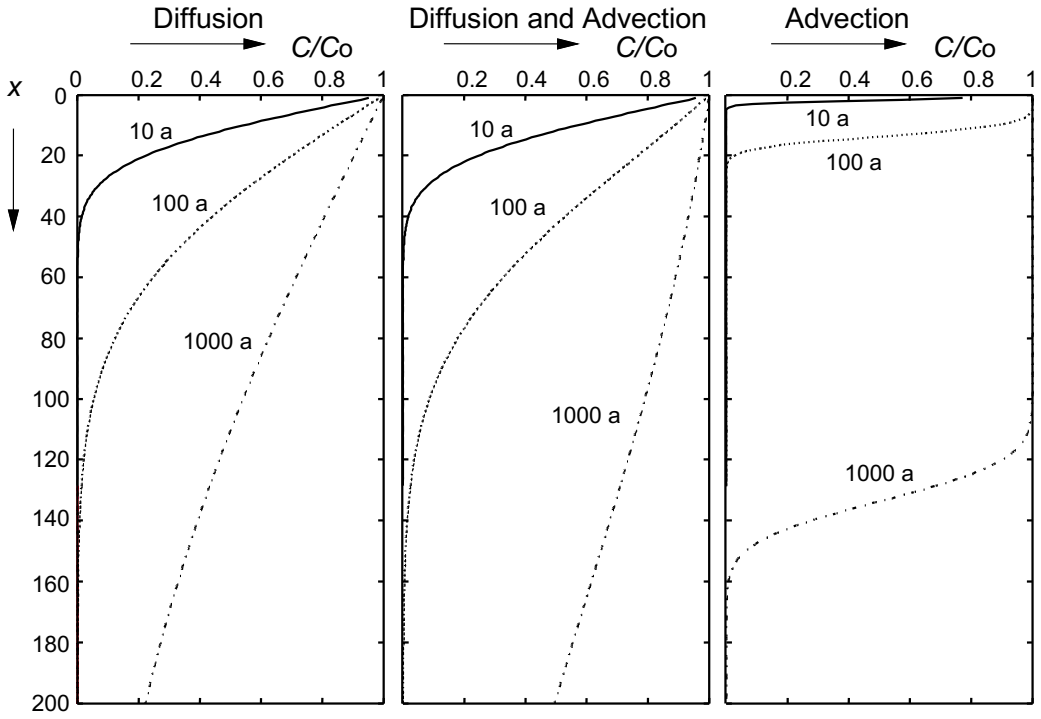

Fig. 7.2: Concentration profiles in a semi-infinite medium calculated for a constant source, assuming pure diffusion (left), advection and diffusion (center) and advection with minor dispersion ($D_l << D_a$). D_e = 1E-06 cm²/s; k_f = 1E-08 cm/s; i = 1; ε = 0.2 (same for diffusion, advection and storage), R = 11.8 ($K_d = 1; d_s = 2.7; D_a = D_e/(\varepsilon\, R) = 8.5\text{E}-07\ \text{cm}^2/\text{s}$).

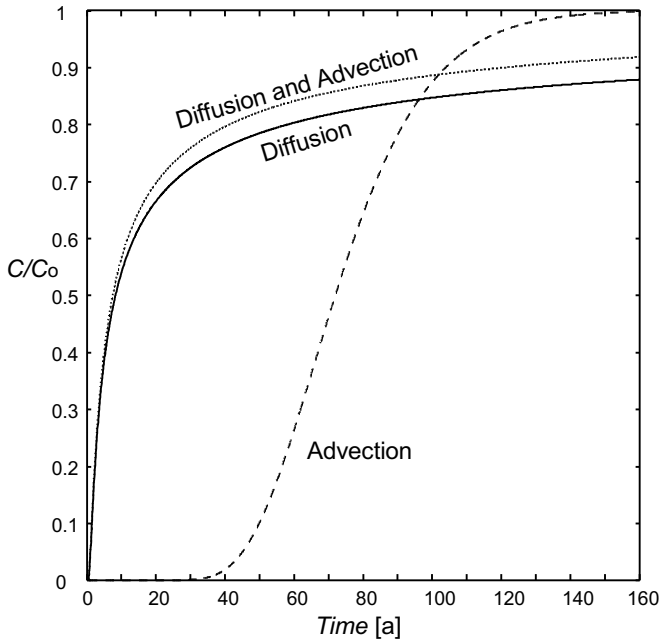

Fig. 7.3: Breakthrough curves at a distance x = 10 cm for the case shown in Fig. 7.2; advection with minor dispersion ($D_l << D_a$)

Box 7.1: A note on "effective" porosities

Depending on the porous medium, sometimes not the total porosity is accessible for transport by diffusion or solute storage; for advection another portion of the pore space may be relevant. This results in different effective porosities in the transport equation:

$$(1-\varepsilon)\rho_{solids}\,K_d\,\frac{\partial C_w}{\partial t}+\varepsilon_{e,s}\frac{\partial C_w}{\partial t}=\frac{D_{aq}\,\varepsilon_{e,t}}{\tau_f}\,\frac{\partial^2 C_w}{\partial x^2}-v\,n_e\frac{\partial C_w}{\partial x}$$

where 4 different porosities appear ($v\,n_e$ is the Dary velocity). ε is the total porosity needed to calculate the dry bulk density ($\rho_b=(1-\varepsilon)\rho_{solids}$) which denotes the dry mass of solids in a unit volume of porous medium ($1-\varepsilon$: volume of the solids, which has nothing to do with any effective porosity). $\varepsilon_{e,s}$, $\varepsilon_{e,t}$, n_e denote a "storage", transport and flow effective porosity, respectively. $\varepsilon_{e,s}$ and $\varepsilon_{e,t}$ may be the same ($=\ \varepsilon_e$) which simplifies the transport equation:

$$\frac{\partial C_w}{\partial t}(\varepsilon_e+K_d\,(1-\varepsilon)\rho_{solids})=\frac{D_{aq}\,\varepsilon_e}{\tau_f}\,\frac{\partial^2 C_w}{\partial x^2}-v\,n_e\frac{\partial C_w}{\partial x}$$

$$\frac{\partial C_w}{\partial t}=\frac{D_e}{(\varepsilon_e+K_d\,(1-\varepsilon)\rho_{solids})}\,\frac{\partial^2 C_w}{\partial x^2}-\frac{v\,n_e}{(\varepsilon_e+K_d\,(1-\varepsilon)\rho_{solids})}\frac{\partial C_w}{\partial x}$$

This leads to two retardation factors:

$$R_{d,diffusion}=1+K_d\,\frac{(1-\varepsilon)\rho_{solids}}{\varepsilon_e}$$

$$R_{d,advection}=\frac{\varepsilon_e}{n_e}+K_d\,\frac{(1-\varepsilon)\rho_{solids}}{n_e}$$

The "classic" R_d for advection is obtained only if $\varepsilon_e=n_e$:

$$R_{d,advection}=1+K_d\,\frac{(1-\varepsilon)\rho_{solids}}{n_e}$$

Note again, the porosity used in the dry bulk density is never "effective" ($\varepsilon_{e,s}$ nor $\varepsilon_{e,t}$ nor n_e)

$\varepsilon_{e,s}$ and $\varepsilon_{e,t}$ may be the same in diffusive transport if e.g. anion exclusion occurs; in mixed layer clay minerals the interlayer water may be accessible for storage but for not for effective solute transport ($\varepsilon_{e,s} > \varepsilon_{e,t}$). In clays $\varepsilon_{e,t}$ may be reduced by the viscoelectric effect which reduces viscosities of water close to solid surfaces. Additionally, anion exclusion may occur , which is relevant, e.g. for disposal of radioactive waste in clay formations.

8. SOME LITERATURE

Adler, P.M., Jacquin, C.G., Thovert, J.-F. (1992): The formation factor of reconstructed porous media. Water Resour. Res., 28, 1571-1576

Archie, G.E. (1942): The electrical resistivity log as an aid in determining some reservoir characteristics. Trans. AIME, 146: 54-62

Aris, R. (1983): Interpretation of sorption and diffusion data in porous solids. Ind. Eng. Chem. Fundam., 22: 150-150

Balberg, J. (1986): Excluded-volume explanation of Archie's law. Phys. Rev. B., 33 (3): 3618-3620

Barr-Howell, B.D., Peppas, N.A., Winslow, D.N. (1986): Transport of penetrants in the macromolecular structure of coals. II. Effect of porous structure on pyridine transport mechanisms. Chem. Eng. Comm., 43 (4-6): 301-315

Bao, Z. Haberer, C., Maier, U., Amos, R.T., Blowes, D.W., Grathwohl, P. (2017): Modeling controls on the chemical weather-ing of marine mudrocks from the Middle Jurassic in Southern Germany. Chem. Geol., 1-12, 10.1016/j.chemgeo.2017.03.021

Bear, J., Nichols, E., Ziagos, J., Kulshrestha, A. (1994): Effect of contaminant diffusion into and out of low-permeability zones. UCRL-ID-115626, Lawrence Livermore National Laboratory, University of California

Beck, R.E., Schultz, J.S. (1970): Hindered diffusion in microporous membranes with known pore geometry. Science, 170: 1302-1305

Bhatia, S.K. (1988): Combined surface and pore volume diffusion in porous media. AIChEJ, 34 (7): 1094-1105

Bruggeman, D.A.G. (1935): Berechnung verschiedener physikalischer Konstanten von heterogenen Substanzen. Ann. Phys., 24: 636-664

Boving, T, Grathwohl, P. (2001): Matrix diffusion coefficients in sandstones and limestones: Relationship to permeability and porosity. J. Cont. Hydrol., 53 (1-2), 85-100

Brusseau, M.L., Jessup, R.E., Rao, P.S.C. (1990): Sorption kinetics of organic chemicals: Evaluation of gas-purge and miscible-displacement techniques. Environ. Sci. Technol., 24: 727-735

Burganos, V.N., Sotirchos, S.V. (1987): Diffusion in pore networks: Effective medium theory and smooth field approximation. AIChEJ, 33: 1678-1689

Carroll, K.M., Harkness, M.R., Bracco, A.A., Balarcel, R.R. (1994): Application of a permeant/polymer diffusional model to the desorption of polychlorinated biphenyls from Hudson River sediments. Environ. Sci. Technol., 28 (2): 253-258

Chantong, A., Massoth, F.E. (1983): Restrictive diffusion in aluminas. AIChE J., 29 (5): 725-731

Charlet, L., Alt-Epping, P., Wersin, P., Gilbert, G. (2017): Diffusive transport and reaction in clay rocks- A storage (nuclear waste, CO_2, H_2), energy (shale gas) and water quality issue. Advances in Water Research (http://dx.doi.org/10.1016/j.advwatres.2017.03.019)

Crank, J. (1975): The mathematics of diffusion, 2nd ed. Oxford, U.K. (University Press)

Crittenden, J.C., Hutzler, N.J., Geyer, D.G., Orawitz, J.L., Friedman, G. (1986): Transport of organic compounds with saturated groundwater flow: model development and parameter sensitivity. Water Resour. Res., 22: 271-284

Currie, J.A. (1960): Gaseous diffusion in porous media. Part I. A non-steady state method. Part II. Dry granular materials. Br. Journ. Appl. Phys., 12: 314-324

Cushman, J.H. (1991): On diffusion in fractal porous media. Water Resour. Res., 27 (4): 643-644

Cussler, E.L. (1984): Diffusion, mass transfer in fluid systems. Cambridge University Press, New York, 525p

Dullien, F.A.L. (1991): Porous Media. Fluid Transport and Pore Structure. Academic Press, 574 p

Dykhuizen, R.C., Casey, M.H. (1989): An analysis of solute diffusion in rocks. Geochim. Cosmochim. Acta, 53: 2797-2805

Epstein, N. (1989): On tortuosity and the tortuosity factor in flow and diffusion through porous media. Chem. Eng. Sci., 44, 777-779

Freeman, D.H., Chang, L.S. (1981): A gel partition model for organic desorption from a pond sediment. Science, 214: 790-792

Frisch, H.L. (1980): Sorption and transport in glassy polymers - A review. Polymer Engineering and Science, 20 (1): 2-13

Grathwohl, P. (1992): Diffusion controlled desorption of organic contaminants in various soils and rocks. 7th International Symposium on Water Rock Interactions, 1992, Park City, Utah, USA

Guegen, Y., Dienes, J. (1989): Transport properties of rocks from statistics and percolation. Math. Geol., 21 (1): 1-13

Heer, W., Haderman, J. (1994): Modelling radionuclide migration - Field experiments. PSI Bericht, Nr. 94-13, Switzerland

Iversen, N., Jørgensen, B.B. (1993): Diffusion coefficients of sulfate and methane in marine sediments: Influence of porosity. Geochimica and Cosmochimica Acta, 57: 571-578
Kärger, J., Ruthven, D.M. (1992): Diffusion in zeolites and other microporous solids. New York (Wiley & Sons, Inc.), 605 p
Kast, W. (1981): Adsorption aus der Gasphase - Grundlagen und Verfahren. Chem. Ing.Tech., 53 (3): 160-172, Weinheim (Verlag-Chemie)
Kast, W. (1988): Adsorption aus der Gasphase. Ingenieurwissenschaftliche Grundlagen und technische Verfahren. Weinheim (VCH), 279 p
Katz, A.J., Thompson, A.H. (1985): Fractal sandstone pores: Implications for conductivity and pore formation. Phys. Rev. Lett., 54 (12): 1325-1328
Kirkpatrick, S. (1973): Percolation and conduction. Rev. Mod. Phys., 13: 574-588
Klinkenberg, I.J. (1951): Analogy between diffusion and electrical conductivity in porous rocks. Geol. Soc. Am. Bull., 62: 559-563
Klotz, W.L., Rousseau, R.W. (1988): Anamolous mass transfer for vapor adsorption on activated carbon. AIChEJ, 34 (8): 1403-1406
Lebedeva, M.I., Fletcher, R.C., Balashov, V.N., Brantley, S.L. 2007. A reactive diffusion model describing transformation of bedrock to saprolite. Chemical Geology, 244, 624–645
Lever, D.A., Bradbury, M.H., Hemingway, S.J. (1985): The effect of dead end porosity on rock matrix diffusion. J. Hydrol., 80: 45-76
Mattes, A. (1993): Vergleichende Untersuchungen zur Sorption und Sorptionsdynamik organischer Schadstoffe (Trichlorethen) in Aquifersanden aus geologisch unterschiedlichen Liefergebieten. Unveröff. Diplomarbeit, Institut für Geologie und Paläontologie der Universität Tübingen
Maxwell, J.C. (1873): A treatise on electricity and magnetism. New York, 1954 (Dover Publications)
Millington, R.J., Quirk, J.P. (1960): Transport in porous media. p 97-106, 7th Intern. Cong. of Soil Science, Madison, 1960
Moldrup, P., Oleson, T., Schjønning, P., Yamaguchi, T., Rolston, D.E., (2000): Predicting the gas diffusion coefficient in repacked soil: Water-induced linear reduction model. Soil Sci. Soc. Am. J., 64, 1588 - 1594
Nicoud, R.M., Schweich, D. (1989): Solute transport in porous media with solute-liquid mass transfer limitations: applications to ion exchange. Water Resources Research, 25 (6): 1071-1082
Nkedi-Kizza, P., Brusseau, M.L., Rao, P.S.C., Hornsby, A.G. (1989): Nonequilibrium sorption during displacement of hydrophobic organic chemicals and 45Ca through soil columns with aqueous and mixed solvents. Environ. Sci. Technol., 23 (7): 814-820
Ogata, A., Banks, R.G. (1961): A solution of the differential equation of longitudinal dispersion in porous media. U.S. Geological Survey Professional Paper, 411-A Washington
Probst, K., Wohlfahrt, K. (1979): Empirische Abschätzung effektiver Diffusionskoeffizienten in porösen Systemen. Chem.Ing.Tech., 1 (7): 737-739, Weinheim (Verlag-Chemie)
Rao, P.S.C., Jessup, R.E., Rolston, D.E., Davidson, J.M., Kilcrease, D.P. (1980): Experimental and mathematical description of nonadsorbed solute transfer by diffusion in spherical aggregates. Soil Sci. Soc. Am. J., 44: 684-688
Rasmuson, A., Neretnieks, I. (1980): Exact solution of a model for diffusion in particles and longitudinal dispersion in packed beds. AIChE Journal, 26 (4): 686-690
Renkin, E.M. (1954): Filtration, diffusion and molecular sieving through porous cellulose membranes. J. Gen. Physiol., 38: 225-243
Reynolds, G.W., Hoff, J.T., Gillham, R.W. (1990): Sampling bias caused by materials used to monitor halocarbons in groundwater. Environ. Sci. Technol., 24 (1): 135-142
Riekert, L. (1985): The relative contribution of pore volume diffusion and surface diffusion to mass transfer in capillaries and porous media. AIChE Journal, 31: 863-864
Rounds, S.A., Tiffany, B.A., Pankow, J.F. (1993): Description of gas/particle sorption kinetics with an intraparticle diffusion model: desorption experiments. Environ. Sci. Technol., 27 (2): 366-377
Sallam, A., Jury, W.A., Letey, J. (1984): Measurements of gas diffusion coefficient under relatively low air-filled porosity. Soil Sci. Soc. Am. J., 48: 3-6, Ann Arbor
Satterfield, C.N., Colton, C.K. (1973): Restricted diffusion in liquids within fine pores. AIChE J., 19: 628
Seidel, A., Carl, P.S. (1989): The concentration dependence of surface diffusion for adsorption on energetically heterogeneous adsorbents. Chem. Eng. Sci., 44 (1): 189-194
Sen, P.N., Scala, C., Cohen, M.H. (1981): A self-similar model for sedimentary rocks with application to the dielectric constant of fused glass beads-. Geophysics, 46: 781-795
Sen, P.N., Scala, C., Cohen, M.H. (1984): Grain shape effect on dielectric and electrical properties of rocks. Geophysics, 49: 586
Shante, V.K.S., Kirkpatrick, S. (1971): An introduction to percolation theory. Adv. Phys., 20: 352-357
Shimamura, K. (1992): Gas diffusion through compacted sands. Soil Science, 153 (4): 274-279

Sing, K.S.W., Everett, D.H., Hanel, R.A.W., Moscou, L., Pierotti, R.A., Rouquerol, J., Siemieniewska, T. (1985): Reporting physisorption data for gas/solid systems with special reference to the determination of surface area and porosity. Pure and Appl. Chem., 57 (4): 603-619

Sontheimer, H., Frick, B.R., Fettig, J., Hörner, G., Hubele, C., Zimmer, G. (1985): Adsorptionsverfahren zur Wasserreinigung. DVGW-Forschungstelle am Engler Bunte Institut der Universität Karlsruhe (TH)

Szecsody, J.E., Bales, R.C. (1989): Sorption kinetics of low-molecular-weight hydrophobic organic compounds on surface-modified silica. J. Contam. Hydrol., 4: 181-203

Taherian, M.R., Kenyon, W.E., Safinya, K.A. (1990): Measurement of dielectric response of water-saturated rocks. Geophysics, 55 (12): 1530-1541

Thoma, G.J., Reible, D.D., Valsaraj, K.T., Thibodeaux, L.J. (1993): Efficiency of capping contaminated sediments in situ. 2. Mathematics of diffusion - adsorption in the capping layer. Environ. Sci. Technol., 27 (12): 2412-2419

Thomas, M.M., Clouse, J.A. (1990a): Primary migration by diffusion through kerogen: I. Model experiments with organic-coated rocks. Geochim. Cosmochim. Acta, 54: 2775-2779

Thomas, M.M., Clouse, J.A. (1990b): Primary migration by diffusion through kerogen: II. Hydrocarbon diffusivities in kerogen. Geochim. Cosmochim. Acta, 54: 2781-2792

Thomas, M.M., Clouse, J.A. (1990c): Primary migration by diffusion through kerogen: III. Calculation of geological fluxes. Geochim. Cosmochim. Acta, 54: 2793-2797

Thompson, A.H., Katz, A.J., Krohn, C.E. (1987): The microgeometry and transport properties of sedimentary rock. Adv. Phys., 36 (5): 625-694

Ullman, W.J., Aller, R.C. (1982): Diffusion coefficients in nearshore marine sediments. Limnol. Oceanagr., 27: 552.556

Van Loon, L. R., Bunic, P., Frick, S., Glaus, M. A., & Wüst, R. A. J. (2023). Diffusion of HTO, ^{36}Cl and ^{22}Na in the Mesozoic rocks of northern Switzerland: I. Effective diffusion coefficients and capacity factors across the heterogeneous sediment sequences. Applied Geochemistry, 159. https://doi.org/10.1016/j.apgeochem.2023.105843

Wagner, N., Balberg, I. (1987): Anamolous diffusion and continuum percolation. J.Stat.Phys., 49 (1/2): 369-382

Wakao, N., Smith, J.M. (1962): Diffusion in catalyst pellets. Chem. Eng. Sci., 17: 825-834

Wang, X.Q., Thibodeaux, L.J., Valsaraj, K.T., Reible, D.D. (1991): Efficiency of capping contaminated bed sediments in situ. 1. Laboratory scale experiments on diffusion - adsorption in the capping layer. Environ. Sci. Technol., 25 (9): 1578-1584

Wang, G., Reckhorn, S.B.F., Grathwohl, P. (2003): Volatilization of VOC from multi-component mixture in unsaturated porous media. Vadose Zone Journal, 692 - 701

Weber, W.J., Smith, E.H. (1987): Simulation and design models for adsorption processes. Environ. Sci. Technol., 21: 1040-1050

Wilson, D.J. (1990): Soil clean up by in-situ aeration. V. Vapor stripping from fractured bedrock. Separation Sci. Technol., 25 (3): 243-262

Wong, P.-Z., Koplik, J., Tomanic, J.P. (1984): Conductivity and permeability of rocks. Phys. Rev. B., 30 (11): 6606-6614

Wong, P.-Z. (1988): The statistical physics of sedimentary rock. Phys. Today, 41 (12): 24-32

Wu, S.C., Gschwend, P.M. (1986): Sorption kinetics of hydrophobic organic compounds to natural sediments and soils. Environ. Sci. Technol., 20 (7): 717-725

Yariv, S. (1976): Organophilic pores as proposed primary migration media for hydrocarbon in argillaceous rocks. Clay Sci., 5: 19-29